Supporting Online Material for

A Global Map of Human Impact on Marine Ecosystems

Benjamin S. Halpern,* Shaun Walbridge, Kimberly A. Selkoe,* Carrie V. Kappel, Fiorenza Micheli, Caterina D'Agrosa, John F. Bruno, Kenneth S. Casey, Colin Ebert, Helen E. Fox, Rod Fujita, Dennis Heinemann, Hunter S. Lenihan, Elizabeth M. P. Madin, Matthew T. Perry, Elizabeth R. Selig, Mark Spalding, Robert Steneck, Reg Watson

*To whom correspondence should be addressed. E-mail: halpern@nceas.ucsb.edu, selkoe@nceas.ucsb.edu

Published 15 February 2008, *Science* **319**, 948 (2008)
DOI: 10.1126/science.1149345

This PDF file includes

Supplementary Online Materials

Methods

General Approach

A comprehensive list of 38 categories of anthropogenic drivers of change in marine ecosystems developed through expert workshops (S*1*) was assessed for data availability on a global scale. We intentionally did not further subdivide these categories into unique drivers (e.g. each specific type of pollutant) as this would lead to over-emphasis of certain activities when impacts are summed. We limited our analyses to anthropogenic drivers with pre-existing global coverage or those for which we could assemble or develop global coverage. Although many regional-scale data and data with a global scope but incomplete coverage exist for a variety of specific human activities, inclusion of these data would bias global comparisons and so were excluded. Anthropogenic drivers that could not be included are, among others: hypoxic zones, coastal engineering (piers, rock walls, etc.), non-cargo shipping (ferries, cruise ships, etc), aquaculture, disease, recreational fishing, changes in sedimentation and freshwater input, and tourism. For all of these drivers data exist for one or more regions, but none have full global coverage. We also assessed availability of global data for 23 different marine ecosystems and were granted access to or developed spatial data for 20 of these. Data that were included in our analyses are listed in Table S1 and described in detail below.

Our cumulative impact model follows a 4-step process (Fig. S1). We first assembled the global data for each anthropogenic driver (D_i) and each ecosystem (E_j). Second, we log[X+1]-transformed and rescaled between 0-1 each driver layer to put them on a single, unitless scale that allows direct comparison, and converted ecosystem data into 1 km^2 presence/absence layers. Third, for each 1 km^2 cell of ocean we multiplied each driver layer with each ecosystem layer to create driver-by-ecosystem combinations, and then multiplied these combinations by the appropriate weighting variable (u_{ij}) These weighting variables come from an expert survey that assessed the vulnerability of each ecosystem to each driver on the basis of 5 ecological traits (S*1*). The weighting values (Table S2) represent the relative impact of an anthropogenic driver on an ecosystem within a given cell when both exist in that cell, and do not represent the relative global

impact of a driver or the overall status of an ecosystem. The sum of these weighted driver-by-ecosystem combinations then represents the relative cumulative impact of human activities on all ecosystems in a particular 1 km^2 cell. Finally, to provide ecological meaning to these relative cumulative impact scores, we used empirical data on the condition of ecosystems to groundtruth our scores. The sensitivity of our results to key steps in this process and further details on the groundtruthing method are provided below. All open-access data and analytical code used in this project can be downloaded at http://www.nceas.ucsb.edu/GlobalMarine.

Data Layers

Land-based drivers

We evaluated the impact of land-based anthropogenic drivers of change on ocean ecosystems with a 4 step process. First, watershed boundaries were developed with an automated flow-accumulation process (S*2*) on the basis of 30 arc-second (nominally 1km^2) SRTM30 Digital Elevation Model (DEM) data (http://glcf.umiacs.umd.edu/data/srtm/) and manually validated against the 391 Global Terrestrial Network for River Discharge (GTN-R) large watersheds (http://gtn-r.bafg.de), VMAP0 stream and river data (S*3*), global coastline data (S*4*), SRTM 3 arc-second DEM data, Landsat imagery, and satellite imagery viewed in Google Earth. These new watersheds represent a significant improvement over the Hydro 1K (http://edc.usgs.gov/products/elevation/gtopo30/hydro/) boundaries and focus on high accuracy for the boundaries of watersheds that reach the ocean and the coastal pour-points for watersheds. Second, data for land-based drivers (nutrient input, non-point source organic and inorganic pollution, and direct impact of humans) were spatially distributed onto the landscape with ancillary data. Nutrient and non-point source organic pollution data came from Food and Agriculture Organization (FAO) national statistics (http://faostat.fao.org) on average annual use of fertilizers (nutrients) and pesticides (organic pollutants) for the years 1993-2002 and 1992-2001, respectively, and were distributed across landscapes in agricultural lands with dasymetric techniques (S*5*). These techniques use ancillary data to distribute values and were developed for mapping human population densities; here the ancillary data were land-use categories from the

U.S. Geologic Survey (http://edcsns17.cr.usgs.gov/glcc/) which identify native, cultivated, and urbanized land uses at 1 km^2 resolution. Non-point source inorganic pollution was modeled with global 1 km^2 impervious surface area data (http://www.ngdc.noaa.gov/dmsp/) under the assumption that most of this pollution comes from urban runoff. These data will not capture point-sources of pollution or non-point sources where paved roads do not exist (e.g., select places in developing countries). Third, values for these three anthropogenic drivers were then aggregated to the watershed and distributed to the pour point (i.e., stream and river mouths) for the watershed with raster statistics (i.e., aggregation by watershed). Finally, spread of the driver values into coastal waters at each pour point was modeled with a cost-path surface (S*6*) on the basis of a decay function that assigns a fixed amount of the driver (in our case, 0.5% of the value in the previous cell) in the initial cell and then evenly distributes the remaining amount of driver in all adjacent and 'unvisited' cells, repeated until a minimum threshold (0.05% of global maximum) is reached. This approach to modeling river plumes is diffusive and so allows drivers to wrap around headlands and islands, but does not account for nearshore advection that acts to push drivers in particular directions. Because nearshore circulation patterns are known for only a few small regions of the world, we conservatively used this diffusive model. Our fourth land-based anthropogenic driver was the direct impact of humans, such as coastal engineering, intertidal trampling and noise pollution from land, which likely scale with population size. This driver was modeled as the sum of the coastal population, defined as the number of people within a moving circular window around an arbitrary focal coastal cell of radius 25 km on the basis of the 2005 LandScan 30 arc-second population data (http://www.ornl.gov/sci/landscan/). This value was then assigned to the adjacent ocean cell since this driver primarily affects intertidal and very nearshore ecosytems.

Ocean-based drivers

Commercial Fishing (5 types)

We identified 5 different categories of commercial fishing gear on the basis of whether or not the gear modifies habitat, if it incurs bycatch, and if it occurs in pelagic or benthic areas (S*7*). Since habitat-modifying fishing is by definition high-bycatch and

habitat-modifying methods for pelagic fishing do not currently exist, five categories of fishing emerge: pelagic low-bycatch, pelagic high-bycatch, demersal habitat-modifying, demersal non-habitat-modifying low-bycatch, and demersal non-habitat-modifying high-bycatch (see Table S4 for lists of gear types in each category). We then used half-degree global commercial catch data developed by the Sea Around Us Project (S*8*) on the basis of data from FAO and other sources. This dataset provides gear type and species caught for all reported fish for the most recent 5 years (1999-2003), which was used to calculate average catch rate (tons per km^2 per year) for each fishing category for each half-degree cell.

These catch-per-area values, per gear category, were then divided by average productivity (g Carbon/m^2/yr) for each cell on the basis of productivity data derived from the Vertically Generalized Production Model (VGPM) (S*9*) to create an estimate of average catch rate standardized by productivity, under the assumption that higher catch rates in lower productivity regions of the ocean have a higher impact than similar catch rates in higher productivity regions. These catch rates were assumed to be uniform within half-degree cells and so all 1 km^2 cells within the larger cell were assigned the productivity-adjusted catch rate for the half-degree cell. Final data for the commercial fishing layers were in units of tons of fish per tons of carbon in each 1 km^2 cell.

We recognize several limitations to our approach. Our assumption of equal impact across all 1 km^2 within each half-degree cell is likely not accurate. Furthermore, the techniques used by The Sea Around Us Project (SAUP) at the University of British Columbia to report catch data at the half-degree resolution, although exposed to strong quality-control measures, also make certain assumptions in order to distribute coarser catch data to the half-degree resolution. As such, our impact scores for any given 1 km^2 cell are estimates from assumptions about the spatial distribution of catch data within regions of the ocean. We also could not account for the population size of species at a location – this value would allow us to truly account for the impact of catch on a location. Our method of adjusting catch by productivity attempts to estimate this standing stock, but is clearly only a proxy measure and may be a poor measure for highly migratory stocks. Finally, we did not account for historical fishing, which has removed vast

numbers of fish in many cases and affected oceans in a way that is not captured by current catch data (S*10, 11*).

Artisanal Fishing

The FAO reports small-scale fisheries data for 59 countries. The Sea Around Us Project (SAUP) subjected these data to initial quality checks (spot validation against locally-derived data) and kindly made these first-draft data available to us. A multivariate regression model was used to isolate geographic, demographic, and socioeconomic variables that best predict the SAUP-validated artisanal catch rates from FAO (excluding values estimated by SAUP). Data for these variables were obtained from the CIA World Factbook (http://www.cia.gov/cia/publications/factbook), World Resources Institute EarthTrends database (http://www.earthtrends.wri.org), and ETOPO2 bathymetric data (http://www.ngdc.noaa.gov/mgg/global/relief/ETOPO2/) and included: length of coastline, shallow shelf area (<100m within EEZ), 2005 population size, proportion of population living within 100 km of the coast, per-capita GDP (calculated as the mean of this value from 2001-2003, in 2006 US dollars), unemployment rates, proportion of total protein supply from fish products, daily per capita consumption of fish and fisheries products, total number of commercial fishing vessels, total annual landings of marine animals taken for commercial, industrial, recreational and subsistence purposes, and the ratio of total landings to total number of commercial vessels.

Data were logit- (for proportional data) and log10- (for all other data) transformed to normalize distributions and the correlation matrix was used to explore relationships among potential predictor variables. Each variable was ranked in terms of the number of missing data (i.e., countries) and this information was used to evaluate how to maximize degrees of freedom in the model. For variables that were highly correlated and measured different aspects of the same characteristic (e.g., seafood consumption, commercial fishing effort), one was dropped from further analyses to avoid potential problems associated with multicollinearity. The variable dropped from such pairs was determined on the basis of the numbers of missing data points and/or the strength of the relationships with the available small-scale catch data. All possible subsets regression (S*12*) was employed to explore all possible combinations of parameters to find the combination(s)

that explained the largest possible fraction of the variance in the empirically-derived artisanal catch data. This procedure uses multiple linear regression to generate rankings for the specified number of possible combinations, which are then statistically evaluated; we used an exhaustive search method instead of forward- or backward-selection procedures to isolate significant predictor variables, as these latter methods are more susceptible to issues of multicollinearity among predictor variables (S*12*). A multiple linear regression model was then run for the smallest set of predictor variables that explained the largest possible fraction of error (R^2). On the basis of this model, fitted values were assigned to their respective countries to generate a full set of predicted annual artisanal landings. The best and simplest model involved only two variables, length of coastline and unemployment rate ($R^2 = 0.79$): $C_T = 10 \wedge (0.33183 + 1.21235(\log10(COASTLINE) + 0.02592(\log10(UNEMPLOYMENT)))$. This model was used to predict artisanal catch values for countries without FAO-reported data.

Finally, we distributed these national total catch values (C_T) into 1 km^2 cells using the following model. The coastal population pressure in each terrestrial cell (see *Land-based drivers*) adjacent to the ocean (P_i) was calculated as the sum of total population within a 25 km radius, which was then used to calculate the fraction of the per-country total population pressure ($T_P = \Sigma P_i$) that fell in that cell (P_i/T_P). The 25 km radius was chosen arbitrarily as a global average distance that artisanal fishers likely travel to get to the coast. This fraction was then multiplied by C_T to estimate the amount of artisanal fishing in a country landed at that cell (C_i). Finally, each nominally 1 km^2 cell within the continental shelf (depth <200m) was assigned a percentage value representing distance from nearest land with inverse distance weighting (IDW), with a power parameter of p = 1.2. These percentage values were multiplied by the C_i value in the nearest terrestrial cell to give a catch-per-cell value. Each cell's value was divided by the sum of values in all cells within a country such that it represented a fraction of the C_T and in turn preserved the sum total catch for each country. This model therefore assumes a strong exponential decay of catch with distance from land within the continental shelf, which we feel is appropriate as most artisanal fishing occurs in small vessels which tend to stay close to shore.

This approach to estimating the impact of artisanal fishing cannot distinguish between methods that do and do not modify habitat. Some developing nations have a high rate of habitat-modifying artisanal fishing and our estimate of the impact of this activity in those locations will be underestimated. Unfortunately, the distribution of habitat-modifying fishing methods is currently unknown in a globally-comparable way. Artisanal fishing is notoriously difficult to estimate (S*13*); our approach uses coarse FAO estimates, models missing national data, and then models the small-scale distribution of national data.

Benthic Structures (oil rigs)

Structures built in the ocean leave a footprint of destroyed habitat where they are built. Such structures include gas and communication pipelines and oil extraction rigs. Data for the former are not freely available, and so we focused on oil rigs as an estimate of the effect of this activity on ocean ecosystems. The Defense Meteorological Satellite Program within the National Oceanic and Atmospheric Administration (NOAA) produces nominally 1 km^2 data on the location of stable lights at night, the Stable Lights of the World dataset (http://www.ngdc.noaa.gov/dmsp). Image and data processing were conducted by NOAA's National Geophysical Data Center (NGDC), with ephemeral sources of lights (e.g. fires, mobile structures) removed. On land, stable lights at night represent human settlements with electricity; in the ocean these stable lights are primarily flares from oil rigs (in contrast to squid and shrimp boat lights which move from night to night or even within nights and produce a different and discernable spectral signal). We focus here on the stable flares data from NGDC, isolated through spectral analysis. We used data from the most recent year, 2003, reported at 30 arc-second (~1 km^2) resolution. We reclassified each cell as presence/absence of light, and clipped the data to the ocean cells.

Commercial Activity (Shipping Lanes)

Commercial shipping activity can lead to ship strikes of large animals, noise pollution, and a risk of ship groundings or sinkings. Ships from many countries voluntarily participate in collecting meteorological data globally, and therefore also

report the location of the ship. We used data collected from 12 months beginning October 2004 (collected as part of the World Meteorological Organization Voluntary Observing Ships Scheme; http://www.vos.noaa.gov/vos_scheme.shtml) as this year had the most ships with vetted protocols and so provides the most representative estimate of global ship locations. The data include unique identifier codes for ships (mobile or a single datum) and stationary buoys and oil platforms (multiple data at a fixed location); we removed all stationary and single point ship data, leaving 1,189,127 mobile ship data points from a total of 3,374 commercial and research vessels, representing roughly 11% of the 30,851 merchant ships >1000 gross tonnage at sea in 2005 (S*14*). We then connected all mobile ship data to create ship tracks, under the assumption that ships travel in straight lines (a reasonable assumption since ships minimize travel distance in an effort to minimize fuel costs). Finally, we removed any tracks that crossed land (e.g. a single ship that records its location in the Atlantic and the Pacific would have a track connected across North America), buffered the remaining 799,853 line segments to be 1 km wide to account for the width of shipping lanes, summed all buffered line segments to account for overlapping ship tracks, and converted summed ship tracks to raster data. This produced 1 km^2 raster cells with values ranging from 0 to 1,158, the maximum number of ship tracks recorded in a single 1 km^2 cell.

Because the VOS program is voluntary, much commercial shipping traffic is not captured by these data. Therefore our estimates of the impact of shipping are biased (in an unknown way) to locations and types of ships engaged in the program. In particular, high traffic locations may be strongly underestimated, although the relative impact on these areas versus low-traffic areas appears to be well-captured by the available data (Fig. S2), and areas identified as without shipping may actually have low levels of ship traffic. Furthermore, because ships report their location with varying distance between signals, ship tracks are estimates of the actual shipping route taken.

Invasive Species (ports)

The incidence of invasive species was modeled as a function of the amount of cargo traffic at a port, on the basis of results from other studies showing a relationship between these two variables (S*15, 16*) and in the absence of actual data for the global

distribution of invasive species. Port volume data (in metric tons, mt) were available for 618 global ports from several sources: the 2002 World Port Ranking (N=36) and 2003 U.S. Port Ranking (N=102) compiled by the American Association of Port Authorities (http://www.aapa-ports.org), Australia ports database (N=30; http://www.aapma.org.au/tradestats; access date 3/19/05), and Lloyds List database [N=450; Ref (S*17*)]. These data are for different years between 1999 and 2003. For 81 ports, multi-year data were available. These multi-year data were used to calculate annual percent change in port volume. Average annual percent change was then calculated for large ports (>50 million mt of cargo, N=18) and smaller ports (<50 million mt of cargo, N=63). These values were used to adjust port volume data for the 618 ports to produce estimated 2003 volumes with values ranging from 11,729 – 350,573,176mt (mean = 3,364,552mt).

The World Port Index (http://www.nga.mil/portal/site/maritime/) lists 4,606 global ports, with details of the types of services available at the port, such as port depth, number of cranes available, train access, etc. The port locations were initially reported to the nearest tenth degree of latitude and longitude; we geocoded the port names with Geonames (http://gnswww.nga.mil/geonames/GNS) to accurately assign port location at the 1 km^2 resolution. The number of services at each port was summed, giving a range of values for each port from 0 to 44. Port volume data from the 618 ports with volume data were regressed against these values and an exponential function (best fit) was fit to the data [$P<0.0001$, $R^2=0.27$]. This relationship was then used to calculate port volume data for the other ~4000 ports. Although this relationship has relatively low explanatory power, it allows for a reasonable estimate of port volume in areas where actual data are not available. Port volume values were input into a model of spread, described below, that was used to calculate a relative measure of risk of invasive species.

To model the spatial impact of invasive species, we used a diffusive plume model to mimic invasion fronts and spread the value for each port at 1 km^2 resolution into adjacent waters, with a minimum threshold value of 5 mt set as a limit to the spread of the plume (i.e., once the value in a cell fell below 5 mt, the plume was assumed to be at its furthest extent). This set a maximum distance from the largest port of 1000 km, an arbitrary but reasonable maximum distance. These areas were then clipped to the shallow

habitats (<60 m depth), since most known invasive species transported by ballast water are intertidal or shallow subtidal.

Our approach to modeling invasive species does not account for species that arrive through other transport mechanisms (such as aquaculture), and it assumes a linear relationship between invasive species occurrence and port volume, and between spatial extent of the invasion and port volume. The former relationship may instead have a threshold value or non-linear relationship, but such relationships are probably taxa-specific and are not currently known for most species. The latter relationship is also not likely to be linear, as the spread of species along coastlines is more likely a function of time since introduction and dispersal capabilities, variables which are available for only a select few marine invasive species, and the relative ocean climatology of the origin and destination of the ship. For example, models that account for the environmental niche of potential invaders perform better than models created solely on the basis of port volume (S*18*), but such niches are not known for most invasive species, and tracking the origin and destination of ships is computationally prohibitive.

Ocean Pollution (Shipping Lanes, Ports)

Ocean-based pollution is assumed to derive from commercial and recreational ship activity. No data on global recreational ship activity currently exist, and therefore we modeled this driver to oceans using a combination of the commercial shipping traffic data (see *Commercial Activity*) and port data (see *Invasive Species*) described above. The shipping data provide an estimate of the occurrence of ships at a particular location, and therefore an estimate of the amount of pollution they produce (via fuel leaks, oil discharge, waste disposal, etc.) that is unique from their contribution to ship strikes, etc. described above. We recognize that ocean currents can disperse this pollution into untraveled regions, but small-scale oceanography is known for only a few select locations around the world, and pollutants are likely to be most concentrated in high traffic areas.

The dispersal of port-derived pollution was modeled as a diffusive plume, like *Invasive Species*, but with a maximum distance of 100 km since the short-term spread of pollutants is likely to span shorter distances than the long-term spread of invasive species. These plumes were not clipped to shallow regions as was done for *Invasive Species*. We

used the shipping traffic data as above, under the assumption that traveling ships primarily affect their immediate waters. The log-transformed and rescaled values from these two layers were summed and rescaled to create a single ocean pollution layer.

Climate change (SST)

Changes in sea surface temperature as a result of climate change will have varying effects on species and ecosystems depending on background temperature variation at a location. Potential for ecological change in response to changes in sea surface temperature can be measured as the frequency of temperature anomalies, where the temperature exceeds a threshold value like the long-term mean, or by a measure of the magnitude (°C) of the anomalies themselves (S*19, 20*). We used 4.6 km (nominally 21 km^2 at the equator) Advanced Very High Resolution Radiometer (AVHRR) Pathfinder Version 5.0 SST data produced by NOAA's National Oceanographic Data Center and the University of Miami's Rosenstiel School of Marine and Atmospheric Science (http://pathfinder.nodc.noaa.gov) to create a global database of temperature anomalies. This database was then used to calculate differences in anomaly frequency between 2000-2005 and 1985-1990.

We first developed a climatology or long-term weekly average for each approximately ~4 km grid cell using data from 1985 to 2005. These data provide a baseline for determining when temperatures are unusually warm. We then developed two metrics for quantifying climate change as a driver of change in marine ecosystems. For our first metric, we calculated the number of times the SST anomaly exceeded the standard deviation of SSTs for that location and week of the year. This threshold-based approach accounts for natural variability at a given location, which can vary widely from place to place, by incorporating the standard deviation. The second metric was the mean SST anomaly temperature value normalized by the standard deviation, a continuous variable approach that also accounts for differences in variability from region to region. The resolution of the temperature data is coarser (21 km^2) than the resolution of analysis (1 km^2); each 1 km^2 cell within the larger cells was assigned the value of the two metrics for the 21 km^2 cell.

These two metrics of SST should be correlated, and indeed they were highly correlated for a test region (45°N-22.5°N, 90°W-67.5°W) in the Western Atlantic and Caribbean that has a wide range of values (linear regression; $R^2 = 0.91$, $P < 0.00001$) and for a random sample of 20,000 cells around the globe (linear regression; $R^2 = 0.998$, $P < 0.00001$; these sub-samples were necessary because the data layers are too large to analyze in their entirety). Consequently, we focused on only the threshold anomaly metric as a measure of SST change for our analyses. We then developed a change metric by subtracting the number of non-zero positive anomalies in the early period (1985-1990) from the number in the recent period (2000-2005); these are the data included in our cumulative impact model.

To test for sensitivity of results to our choice of focal years (2000-2005), we used the Western Atlantic and Northern Caribbean as a test region to compare values for the past 10 years (1995-2005) and the entire dataset (1985-2005) for both metrics describe above. If mean and variance values are increasing over time, then one should see decreasing fits in the data with an increasing span of time being compared. Indeed, all comparisons were highly significant ($P<0.00001$) with high but decreasing R^2 values when the most recent data were compared to the entire dataset, the past 10 years, and the most recent period (linear regression; anomalies 5 yrs vs. 10 yrs $R^2 = 0.961$, 5 yrs vs. 20 yrs $R^2 = 0.93$; normalized means 5 yrs vs. 10 yrs $R^2 = 0.9997$, 5 yrs vs. 20 yrs $R^2 = 0.9993$). Our approach did not account for potential presence of thermo-tolerant species or local-scale oceanography that could modify how resistant a local ecosystem is to changes in SST.

Climate change (UV)

The intensity of ultraviolet (UV) radiation reaching the surface of Earth was measured from August 1996 to July 2004 as part of the GSFC TOMS EP/TOMS satellite program at NASA. These data have been processed by NASA to isolate the amount of erythemal UV light (the UV-B spectrum of UV light that is most harmful to organisms; 315-280 nm wavelength) that reaches Earth's surface (data available at http://iridl.ldeo.columbia.edu/SOURCES/.NASA/.GSFC/.TOMS/.EPTOMS/.monthly/.uv/) (S*21*). Data are reported as the average Joules (J) per m^2 per month at one-degree cell

(~110 km by 110 km) resolution for the areas between 65°S to 65°N. We used these data to calculate the climatological mean and standard deviation of erythemal UV light reaching each 1-degree cell for each month. Our measure of anomalously high values (i.e., a potential response to climate change) was the number of times between 2000 and 2004 that the monthly average exceeded the climatological mean + 1 standard deviation. These values were summed across the 12 months to provide a single value, ranging from 0-19, representing the number of anomalous values in that particular location over the entire 5 years. We did not use the metric of change in these anomalous values from the early period to the current period, as was done for SST data, since the entire UV dataset covers only 9 years.

As with SST data above, our approach to modeling the impact of changing UV on ecosystems assumes equivalent impacts within and among different regions. Local factors such as small-scale shading and oceanography and the presence of UV-resistant species may help make some locations more tolerant than others. The data also only span 9 years, so historical levels of UV, against which to compare current levels, are not known. However, if the strong correlation between SST anomaly values for recent and historic years (see above) is generalizable, the UV results for the most recent years are likely an adequate measure of spatial variance in the impact of UV on current ecosystems. These data also do not include polar regions and so cumulative impact scores in these regions will be slightly underestimated, however most of the southern polar region is land (Antarctica) and much of the northern polar region is covered in ice for much of the year where we do not calculate cumulative impact scores.

Climate change (acidification)

Changes in CO_2 concentration alter the aragonite saturation state (ASS) of the ocean, among other chemical properties of seawater, and as ASS levels drop the ability of calcifying species such as corals and shelled invertebrates to create calcium carbonate structures declines (S*22*). The global distribution of ASS values has been modeled at 1-degree resolution for pre-industrial (circa 1870) and modern times (2000-2009) (S*23*). We use the difference between these values as an estimate of the human-derived driver of changes in ocean acidification.

Normalization of driver data layers

Nearly all of the anthropogenic driver data had extreme left-skewed distributions with very small numbers of extremely high outlier data. The extreme outlier data may or may not be precisely accurate, and so we sought to minimize the impact of this potential source of error on our model results. To do so we log[X+1]-transformed each data layer, except *benthic structures*. *Benthic structures* were treated as binary data since presence of an oil rig is an all-or-nothing event. All data layers were then rescaled between 0-1, with the highest log-transformed value for each driver set = 1. The transformation of data appropriately reduces the effect of extreme outliers when rescaling the data to assign the relative impact of different levels of the anthropogenic drivers considered here (S*24*), while rescaling allows for direct comparison among drivers with dramatically different native scales and units of impact. We also rescaled all driver layers without log-transformation of the data for comparison. This method preserves the true relative magnitude of the data; we found no qualitative differences in our results (not shown) and so focus on those that derive from log-transformed data. Our approach assumed a linear relationship between driver magnitude and impact on ecosystems. This assumption ignores thresholds that likely exist but are known for very few driver-by-ecosystem combinations, but it allows for direct comparison between and among drivers.

Ecosystem Maps

Global data for marine ecosystems are largely non-existent; here we used available data for several ecosystems, modeled the distribution of many other ecosystems, and assumed a uniform distribution for several intertidal ecosystems for which no data exist. We recognize that differences exist in how people classify ecosystems; for example, estuaries are often considered an ecosystem, but here we focus on the ecosystems (also often labeled 'habitats') that occur within estuaries (salt marsh, intertidal mud, beach, soft sediment, mangroves, etc.). All ecosystem data were represented at 1 km^2 resolution.

Hard and Soft bottom shallow, shelf, slope, and deep (8 ecosystems):

The Institute of Arctic & Alpine Research at the University of Colorado at Boulder has collected all available data from benthic substrate point samples, including scientific and industry grab samples, trawls, and core samples, on the rock composition of particular locations around the world as part of the dbSEABED project (http://instaar.colorado.edu/~jenkinsc/dbseabed/). At the time of our purchase of these data (June 2005), the database included 544,543 individual measurements of the percent hard or soft sediment type. The spatial distribution of the data was highly heterogeneous (see Fig. S3), and roughly 65% of the data were 100% soft sediment. Samples with greater than 50% hard substrate were counted as hard; all others were counted as soft. Grid cells were sampled at 2 arc-minutes (~3.7 km, or 13.69 km^2 per cell, depending on latitude) and each cell was assigned a binary value of hard or soft substrate. This resolution was used to match the ETOPO2 bathymetry data.

We then used kriging to classify unsampled locations as either soft or hard on the basis of the distribution of substrate types in the surrounding area. Kriging is a statistical interpolation technique for spatial data that uses the spatial variogram of nearby data to assign values to empty cells (S*25*). Given the vast size of this database, it was not possible to calculate a single variogram for the entire planet, and so we developed variograms for six data-rich regions of the world (Alaska, Florida, Mediterranean, Great Barrier Reef, the North Sea, and New England) and evaluated the kriging solutions that resulted from each of these variograms for indications of poor interpolation, most notably large areas modeled from a single datum and parabolic fan shapes around clusters of points. We used the variogram that resulted in the fewest of these indicators (from the Florida region) and that was from evenly-distributed data that lay along an unbroken swath of coastline with uniform orientation (which reduces clashing trends in the variogram) to produce maps of hard and soft bottom benthic habitats in four different depth ranges – shallow (0-60 m), shelf (60-200 m), slope (200 – 2000 m), and deep/abyssal (>2000 m; Fig. S4. Bathymetry data came from ETOPO2 (2 min. resolution).

Because the distribution of sampling is geographically uneven, some areas of the globe have higher error rates. For example, much of the Southern Ocean is only sparsely sampled in the original point dataset (Fig. S3), and so the kriged data layers for

ecosystems in this region have greater errors than for other areas of the globe. In general, shallow and shelf areas are better sampled than continental slopes and deep seafloor, and regions around developed nations (e.g. in North America, Australia and Europe) are better sampled than those around developing nations. In addition, the data may reflect the tendency for trawlers and others sampling the seafloor to avoid hard substrate. Indeed, ~80% of the samples in the original dataset were categorized as soft (~15% mixed-type substrate and 65% entirely soft-sediment), a likely overestimate of the amount of soft substrate on the ocean floor. Accordingly, we anticipate that the distribution of hard substrate will be under-predicted by this method. Given that soft substrates generally tend to be less vulnerable to anthropogenic drivers of change than hard substrates, this method will be conservative with respect to overall impact levels.

Coral Reefs

The global coral reef atlas (S*26*), compiled by the World Conservation Monitoring Centre at the UN Environment Programme (UNEP-WCMC), combines a large number of coral reef maps deriving from various sources (http://www.unep-wcmc.org/marine/coralatlas/). Quality of the final product is limited by quality of the input cartographic sources, some of which are rather coarse scale. Only 30% of reefs in the atlas were mapped from source data with a resolution of 1:250,000 or higher. Nonetheless, coral reefs represent one of the best global marine habitat datasets and this data layer has been widely vetted and used in marine conservation and science [e.g. (S*27*)]. The data were provided to us by UNEP-WCMC as presence/absence for each $1km^2$ cell; we then clipped these data to our land-sea mask (Table S5).

Seagrass beds

We used UNEP-WCMC's global atlas of seagrasses (S*28*) to represent distribution of this habitat (http://www.unep-wcmc.org/marine/seagrassatlas). The dataset represents a compilation of aerial maps and point records of seagrass occurrence from around the world. Because of the heterogeneous nature of the input data and the large number of point data in the dataset, the spatial accuracy of the seagrass data layer is limited. In addition, many parts of the world have not been comprehensively surveyed

for seagrasses, so this dataset underestimates the distribution of seagrass habitat. Data were overlaid on a 1 km^2 grid and cells were assigned presence or absence of seagrass beds and then clipped to the land-sea mask (Table S5).

Mangroves

Mangrove habitats were mapped with the global mangrove atlas (S*29*) produced by UNEP-WCMC (http://bure.unep-wcmc.org/imaps/marine/mangroves). Like the other UNEP-WCMC products, this dataset is a compilation of multiple cartographic sources, derived from aerial imagery, remote sensing, on the ground surveys and expert opinion. This dataset is considered more accurate that the seagrass dataset (i.e., more entries are polygons instead of points). Nonetheless, mangroves have not been surveyed comprehensively across the globe. Furthermore, when we intersected the mangrove layer with our global coastline layer to eliminate mangroves that fell on land, a large portion of the habitat was lost (Table S5), and there is some error in the original mangrove data. Only 22,139 cells remained globally containing mangrove. Potential errors in processing this data layer will have a minor effect on global results, because of the small number of cells, but this suggests caution in drawing conclusions about global and regional status of mangrove ecosystems. These data were overlaid on a 1 km^2 grid and cells were assigned presence or absence of mangroves.

Surface Water

Pelagic surface waters were mapped as the top 60 m of the ocean in all areas deeper than 60 m total depth. Actual depth of this layer can vary from a few meters in turbid water up to 200 m in highly oligotrophic waters (i.e., most of the open ocean) but is commonly shallower in coastal waters where primary productivity (and therefore turbidity) is greater. We used 60 m to be inclusive. The choice of this depth will only affect the distribution of this ecosystem in coastal waters, and this is also where slight inaccuracies may exist due to variation in the quality of the underlying bathymetric data used to map the 60 m depth contour. The water column over shallow (<60 m) locations was excluded because we assumed that the entire shallow water column acts roughly as a single (benthic-associated) ecosystem.

Deep Water

Pelagic deep waters were defined as the water column from 60 m depth down to the benthos. Like pelagic surface waters, this habitat layer is well mapped, though slight inaccuracies may have been introduced by errors in the bathymetry along the 60 m depth contour. Surface and deep pelagic water habitats are completely overlapping in the horizontal dimension.

Seamounts

Seamount location data came from other research efforts (S*30*) that used ETOPO2 bathymetric data to model seamount location. This research identified peak seafloor anomalies with D8 flow models (S*2*) and then compared the output from two different seamount definitions – peaks with >1000 m rise and peaks with roughly circular or elliptical in shape. The former definition focuses on eliminating small peaks that may not be seamounts, and the latter definition focuses on eliminating peaks along steep ridges (e.g. continental slopes). Overlap of these two models produced 14,287 seamounts globally, estimated to represent roughly 30% of likely seamounts in the world (depending on how one defines seamounts) (S*30*). These data were provided to us as the center of each seamount at 1 km^2 resolution (Fig. S5). To better estimate the spatial coverage of these seamounts, we created a small circular buffer around each point, such that each seamount was represented as five 1 km^2 cells centered on the original points and radiating in the cardinal directions.

Nearshore ecosystems with assumed distributions

Several coastal and intertidal ecosystems currently have no global data on their spatial distribution but are important for understanding the cumulative impact humans are having on the oceans. We included these ecosystems in our cumulative impact model by assuming that rocky intertidal, beach, intertidal mud, suspension-feeding reefs, and salt marsh ecosystems existed in all cells within 1km of shore, and that kelp forest ecosystems exist within all areas <60m deep within their possible range limits (S*31*). We could not include similar range constraints for salt marshes and suspension-feeding reefs

because no published records exist for their global ranges. Consequently, cumulative impact scores for the coastal cells immediately adjacent to the land will likely be overestimated in many cases; we repeated analyses with these ecosystems removed (see below) to test the sensitivity of our results to their inclusion.

Data representation and projection

To create a uniform coastline (land-sea interface) against which we compared all driver and ecosystem data, we used the SRTM30-PLUS data (http://topex.ucsd.edu/WWW_html/srtm30_plus.html) that represents merged SRTM30 and ETOPO2 data. Land-based data that occurred within the ocean or ocean-based data that occurred on land, in reference to this data mask, were clipped and removed. This issue emerges solely for coastal cells, where a $1km^2$ region has both land and ocean in it but must be assigned a binary value (land or ocean) or where the two layers do not meet (i.e. a gap exists). Our approach of applying a uniform land mask ensured consistency across all data used in our analyses, but removed or added area from coastal marine ecosystems (Table S5). Shallow soft bottom and rocky reef ecosystems gained area as a result of this process due to the need to fill gaps between land and ocean datalayers – we expanded neighboring ocean substrate data into these gaps. In contrast, coral reef, mangroves, and seagrass ecosystems lost area since these habitats are in very shallow water and so were more prone to being classified as land. In particular, most area was lost from the mangrove data layer.

All data were represented at $1km^2$ resolution, even though several layers had native resolutions at coarser scales. In doing so, we assumed the coarse-scale value was evenly distributed across all $1km^2$ cells within that region. For the climate change drivers (UV anomalies, SST change, and changes in ocean acidification), this assumption is reasonable given the scale at which those drivers act. The land-based drivers, human population data, and oil/gas development data were all at our native 1 km^2 resolution, and spread of these data into the ocean at the same resolution is reasonable. Regardless, when coarse-scale data are distributed equally to all 1 km^2 cells within the larger area, the coarser scale pattern is essentially recreated while the finer resolution information is preserved where and when it is appropriate. Finally, prior to all analyses, we converted

all data to the WGS84 Mollweide projection as it is an accurate single global projection that preserves area and allows data transfer and analysis among operating systems and software.

Ground-truthing the impact scores

To translate our cumulative impact scores into estimates of ocean condition, we used linear regression to compare estimates of the current condition of 16 regions containing coral reefs from around the world (S*32*) to the average cumulative impact score from our analyses for all cells containing coral reefs in those regions (we had to exclude Moreton Bay because our coral reef data did not have corals present at that location). The published estimates of ecosystem condition (S*32*) were from the relative abundances of a suite of species that use a variety of ecosystem types in and around coral reefs, as well as corals and seagrasses themselves, and so we compare the ecosystem condition values to our cumulative impact scores for the collection of ecosystems in cells containing coral reefs within the regions of analysis. Because the species evaluated (S*33*) were largely subtidal, with the exception of sea turtles that use beaches for nesting, we used the cumulative impact scores that excluded the intertidal ecosystems for which we had to assume uniform coastal distributions (rocky intertidal, intertidal mud, beach, and suspension-feeding reefs, salt marsh) and kelp forests because they have weak or no connection in most cases to the species measured. With the remaining 14 ecosystems, we found a strong positive relationship between cumulative impact score and ocean condition ($R^2 = 0.63$, $P = 0.001$; Fig. S5A). We used the linear regression equation (cumulative impact = 0.1762*(% impacted) - 0.3381) to translate our impact scores into categories of ocean condition, building on a previous classification scheme (S*10, 33, 34*) and on the basis of the necessary assumption of our analytical approach that cumulative impact scores (summed across ecosystem types accounting for differences in vulnerability) can be directly compared between any two locations on the planet. We then used these bins of cumulative impact scores for describing the global condition of marine ecosystems and for color-coding all figures. We recognize that estimates of ocean condition (S*32*) have been criticized (S*35*), but they are one of the few empirically derived, global-scale estimates that exist .

We repeated the above analyses for coral reefs alone to provide an estimate of the relative condition of specific ecosystems. The regression was significantly positive (R^2 = 0.56, P = 0.001) with cumulative impact = 0.065*(% impacted) - 0.76. We used this equation to categorize the relative condition of coral reefs, giving the following threshold values for categories of impact (very low impact = <1.4, low impact = 1.4 – 2.7; medium impact = 2.7 – 4.0; medium high impact = 4.0 – 5.3; high impact = 5.3 – 6.6; and very high impact = > 6.6). We did not apply this equation to other ecosystems as it is not likely to apply to them.

Sensitivity Analyses

Weighting matrix

Methods for assessing the relative impact of drivers are still evolving (S*1*), with our weighting values offering one possible estimate derived from a large group of international marine experts. When these experts were surveyed to determine relative impact scores we did not know which data (or proxy data) would be available for each driver category, and so their responses may not be directly relevant to the data we used here. To test the sensitivity of the resulting cumulative impact scores to the weighting values (Table S2), we conducted Monte-Carlo simulations using randomly shuffled weighting matrices. This method exactly preserves the modes and distribution of the weighting values in the matrix. We ran 500 simulations and used these runs to calculate 95% CIs for global statistics on the amount of ocean that falls into each category of impact (Table S6); mean and variance of these statistics stabilized by N = 200. Results with weighting values from the expert survey were very similar to simulated values, with values slightly but significantly different from null expectations for the categories of very low, medium, medium high, and very high impact (Table S6).

Ecosystem layers

Global cumulative impact scores were recalculated with the 6 ecosystems removed for which distributions were assumed (rocky intertidal, beach, intertidal mud, salt marsh, suspension-feeding reefs, and kelp forests). Results were qualitatively similar globally (R^2 = 0.94 between model outputs with and without these ecosystems) but with

lower cumulative impact scores in nearshore ocean cells, as would be expected since all of these ecosystems are coastal, particularly for those cells immediately adjacent to land (Fig. S6).

Cumulative impact model

Ideally a cumulative impact model would be based on extremely high resolution ecosystem data that would allow for accurate area-based weightings in cumulative impact scores. These data do not exist. Our approach summed impact scores across all ecosystem types within a cell. This approach may overweight predicted human impact on cells with more ecosystems where ecosystems cannot overlap (i.e., they are actually spatially distinct within a cell). We tested an alternate cumulative impact model based on the average driver-by-ecosystem impact scores rather than the sum. We found a very high correlation between outputs of the summed vs. average models ($R^2 = 0.95$), showing that the spatial pattern of relative impact is very similar under either model. There was also a positive correlation between the average cumulative impact scores and ocean condition in the groundtruth regions ($R^2 = 0.46$). Using the new regression equation from this groundtruth correlation led to very similar percents of the ocean in each impact category compared to the summed model: very low impact (14.7%), low impact (20.5%), medium impact (27.4%), medium high impact (31.5%), high impact (4.7%), and very high impact (1.2%).

We used the summed model for the following reasons. Most of the ocean is 3-dimensional with fully overlapping ecosystems when the ocean is viewed in 2-dimensions (e.g. benthic, deep water, and pelagic ecosystems co-occur completely within each cell >60m depth), making the summed model most appropriate for representing impact on this area in a 2-dimensional map. This area of ecosystem overlap accounts for 97.4% of the world's oceans. Furthermore, half (49%) of the remaining coastal area (<60m) has only a single ecosystem, such that the average and sum models produce identical cumulative impact scores in these areas. For the remaining ~1.3% of the ocean where ecosystems coexist within a $1km^2$ cell but may not overlap, reasonable arguments exist for either the average or sum model. For shallow cells with multiple ecosystems, ecosystem type should be spatially unique at the finest resolution (e.g., m^2), such that no

two ecosystems overlap. As resolution becomes coarser, ecosystems are much more likely to overlap, with an intermingled matrix of ecosystem types emerging. Furthermore, cells with multiple ecosystem types may provide greater ecological value, as the ecological connections among them and to the larger region can often be greater than the sum of the parts (e.g., by providing greater biodiversity), and so it is reasonable to weight more the degradation or loss of such cells. For simplicity and consistency, we used a single summed model for the whole ocean.

Supplementary Figure 1. Flow diagram of modeling approach for calculating cumulative impact of human activities on marine ecosystems. Anthropogenic driver data are first log-transformed and then rescaled 0-1. Where driver and ecosystem data overlap, a vulnerability weighting variable is applied and all weighted layers are summed to create a cumulative impact map. Groundtruthing with empirical estimates of ecosystem condition provides an estimate for how impacted oceans are. Driver layers can also simply be summed, but one loses the information on ecosystem-specific vulnerabilities, which clearly emerge in the other model figures.

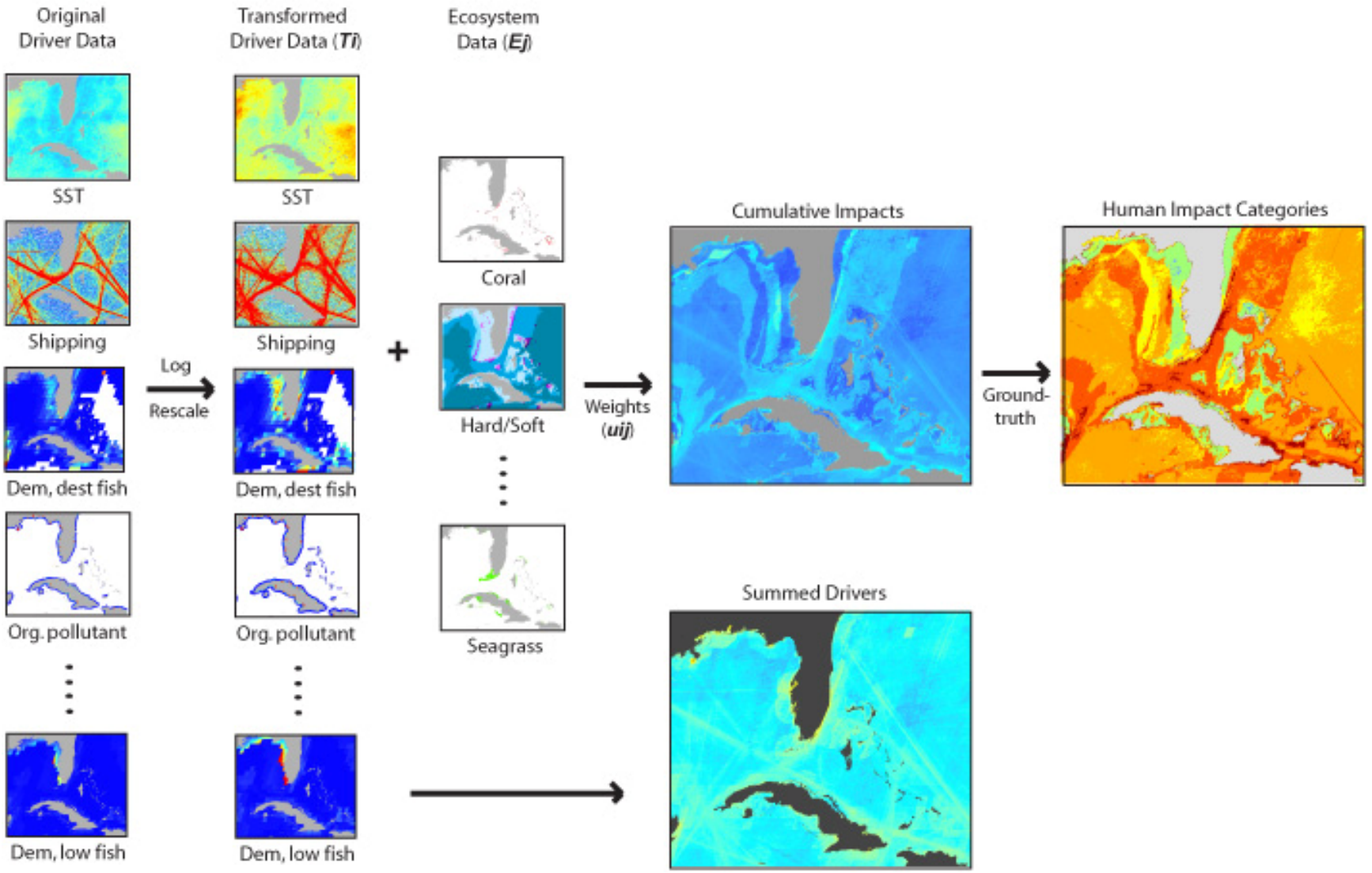
Original Driver Data
Transformed Driver Data (Ti)
Ecosystem Data (Ej)
SST
Shipping
Dem, dest fish
Org. pollutant
Dem, low fish
Log
Rescale
SST
Shipping
Dem, dest fish
Org. pollutant
Dem, low fish
+
Coral
Hard/Soft
Seagrass
Weights (uij)
Cumulative Impacts
Ground-truth
Human Impact Categories
Summed Drivers

Supplementary Figure 2. Global maps of each driver layer (or regional maps, when not visible at global scale) used in analyses: A) pelagic, low-bycatch fishing, B) pelagic, high-bycatch fishing, C) demersal habitat-modifying fishing, D) demersal non-habitat-modifying, low-bycatch fishing, E) demersal non- habitat-modifying, high-bycatch fishing, F) shipping, G) nutrients (Western Mediterranean), H) organic pollutants (Western Mediterranean), I) inorganic pollutants (Western Mediterranean), J) direct human impact (Western Mediterranean), K) artisanal fishing (central Indonesia), L) oil rigs (Gulf of Mexico), M) invasive species, N) ocean pollution, O) sea temperature changes, P) UV changes, and Q) ocean acidification. Images are color-ramped using a normalization process based on 2 standard deviations, where blue denotes low value, red is high value, and white denotes zeroes.

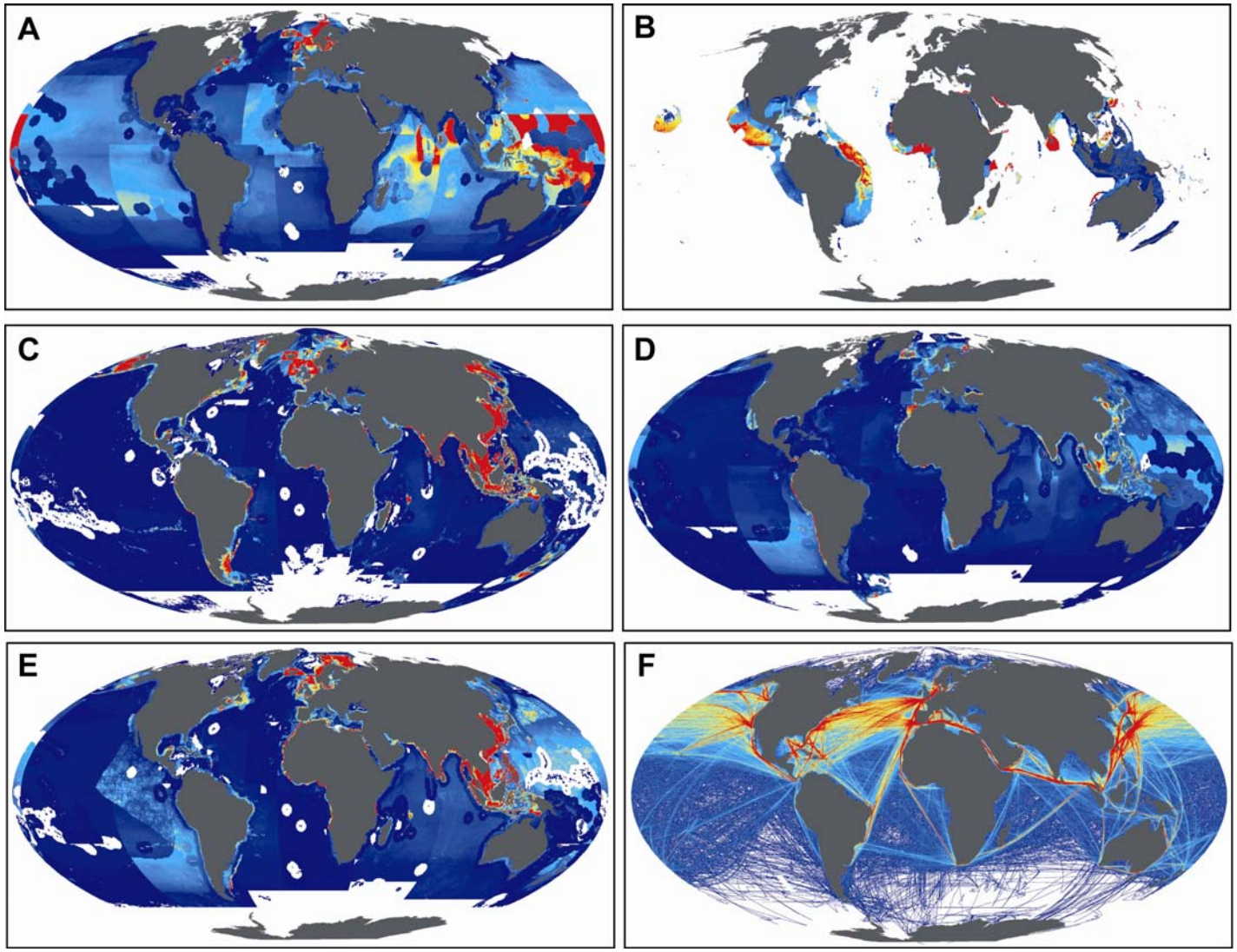
A
B
C
D
E
F

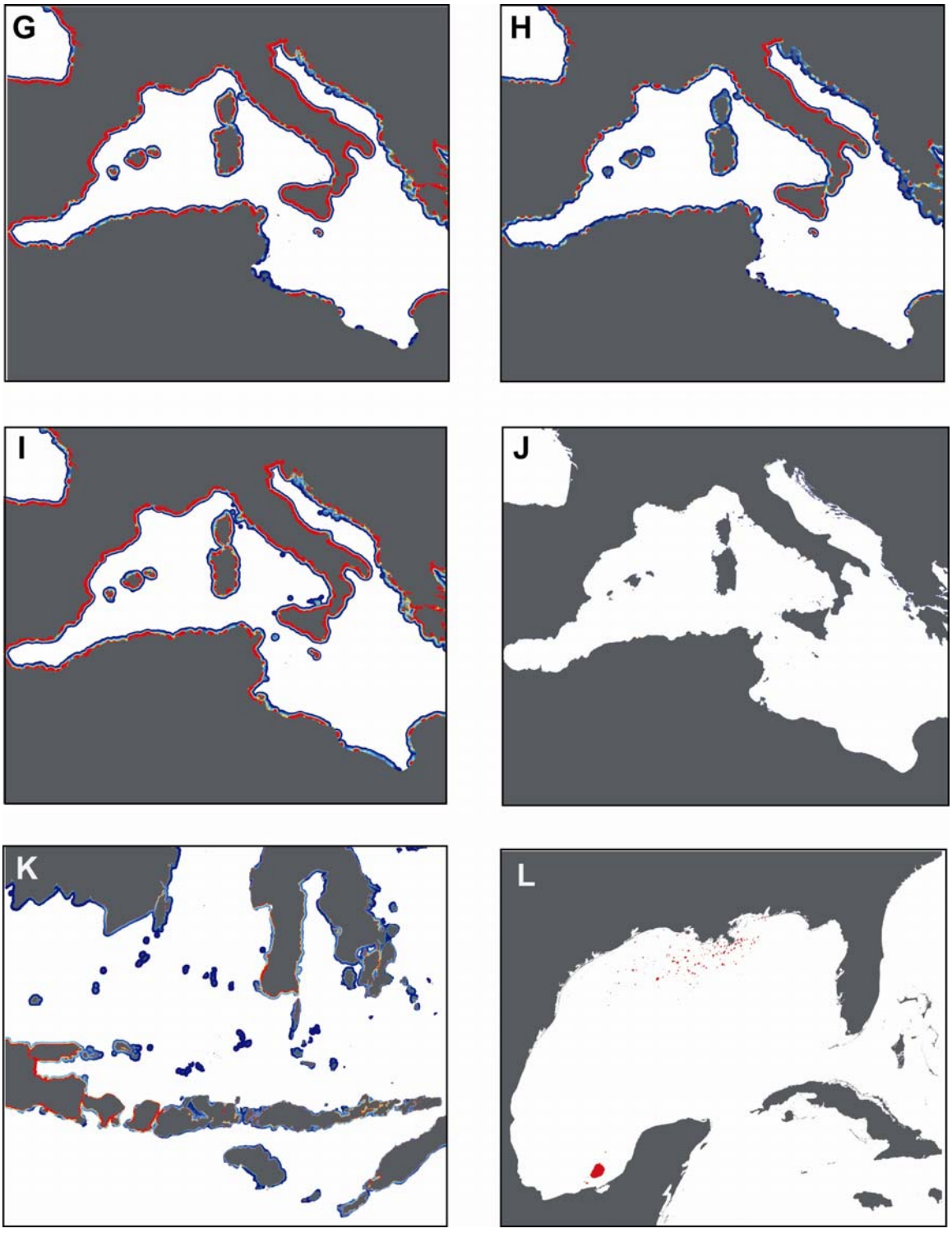
G
H
I
J
K
L

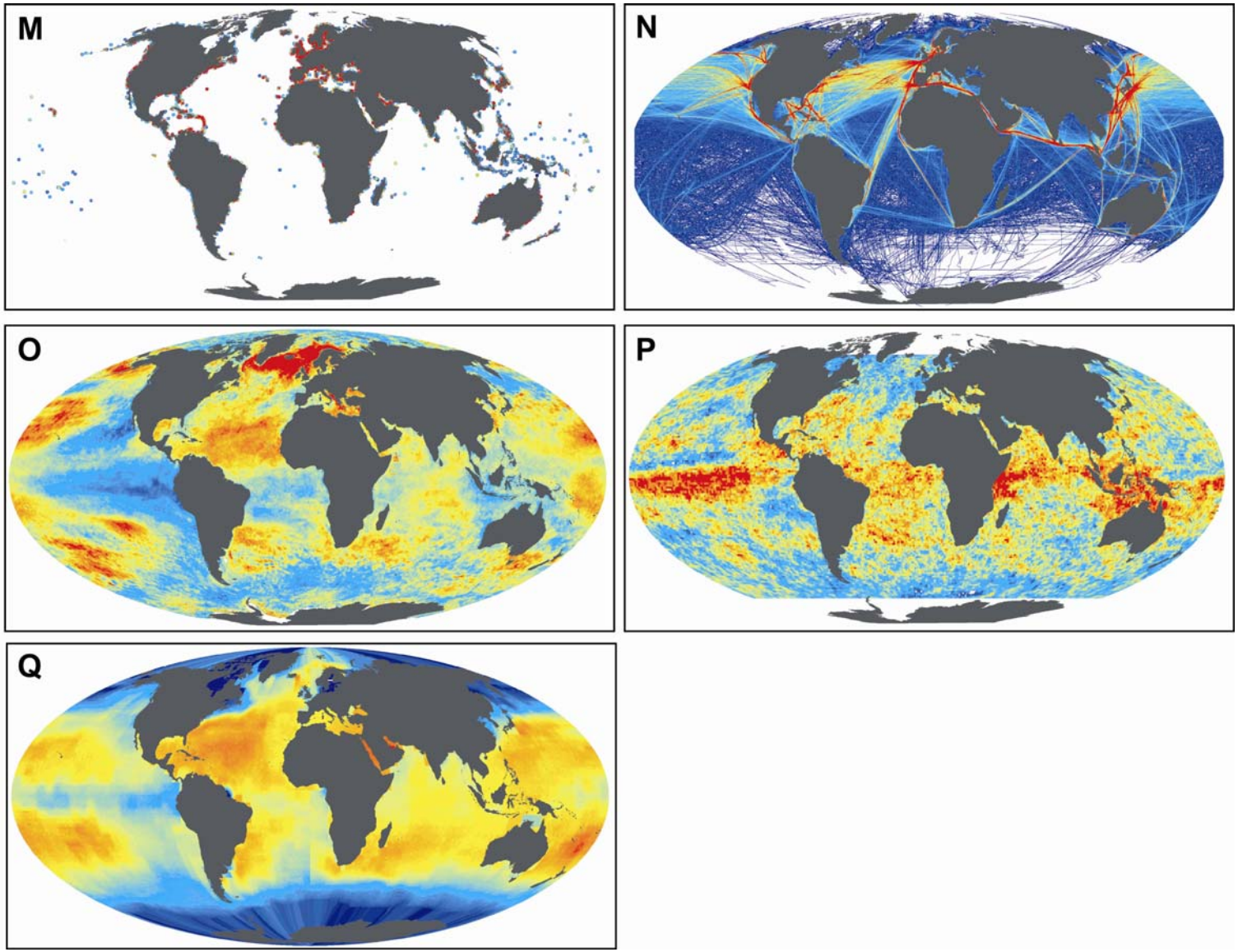
M
N
O
P
Q

Supplementary Figure 3. Global maps of each ecosystem layer used. A) hard and soft shallow, shelf, slope, and deep ecosystems, with soft ecosystems in blue and hard ecosystems in purple and darker colors for deeper ecosystems, B) pelagic surface waters, C) deep waters, D) seamounts, and representative regions of coral reefs (red) and seagrass beds (green) in E) the Western Caribbean and F) Indonesia and Australia, and G) mangroves (purple) in Cuba (these three ecosystems cannot be seen in global projections).

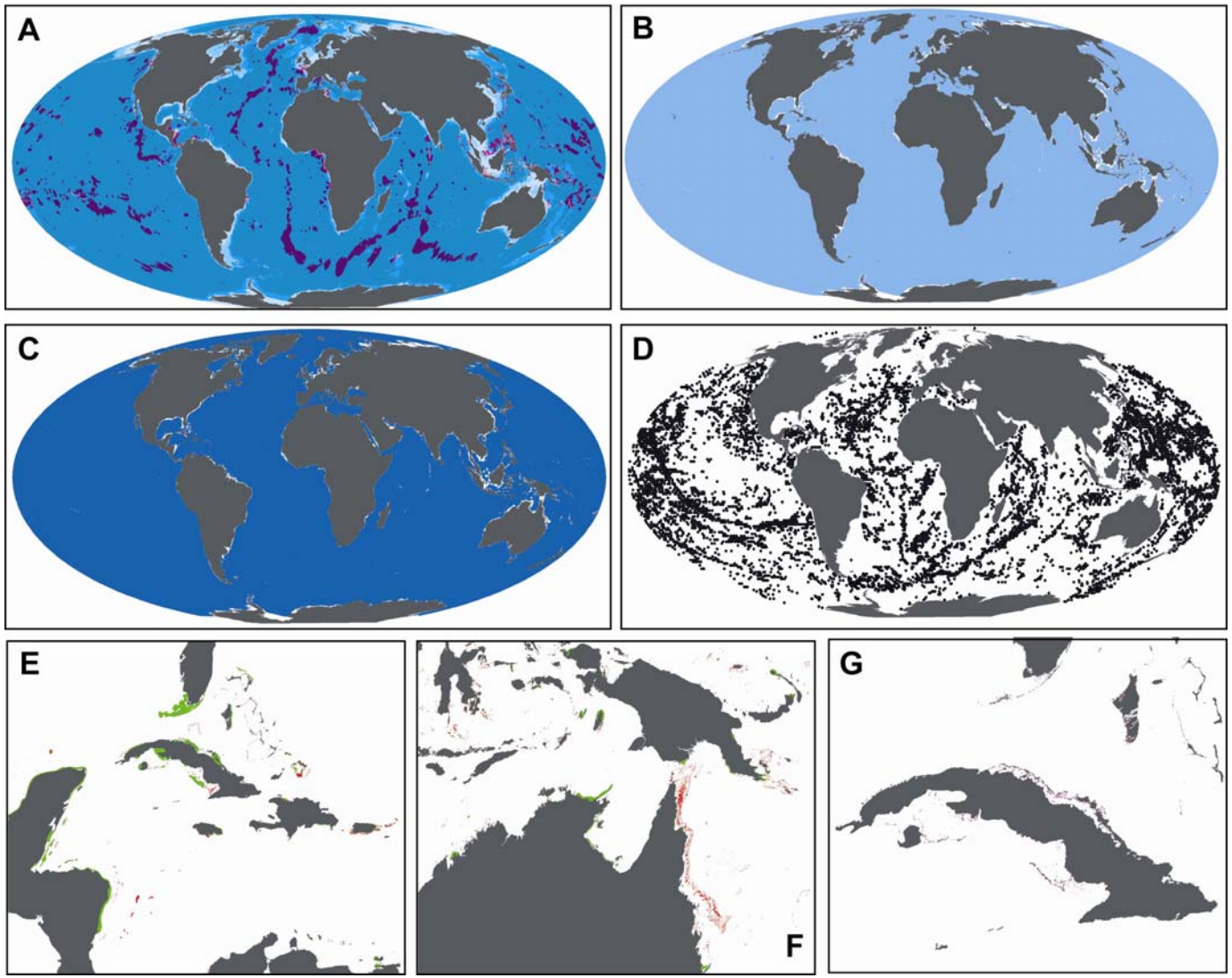
A
B
C
D
E
F
G

Supplementary Figure 4. Location of the benthic substrate composition data from the dbSEABED project.

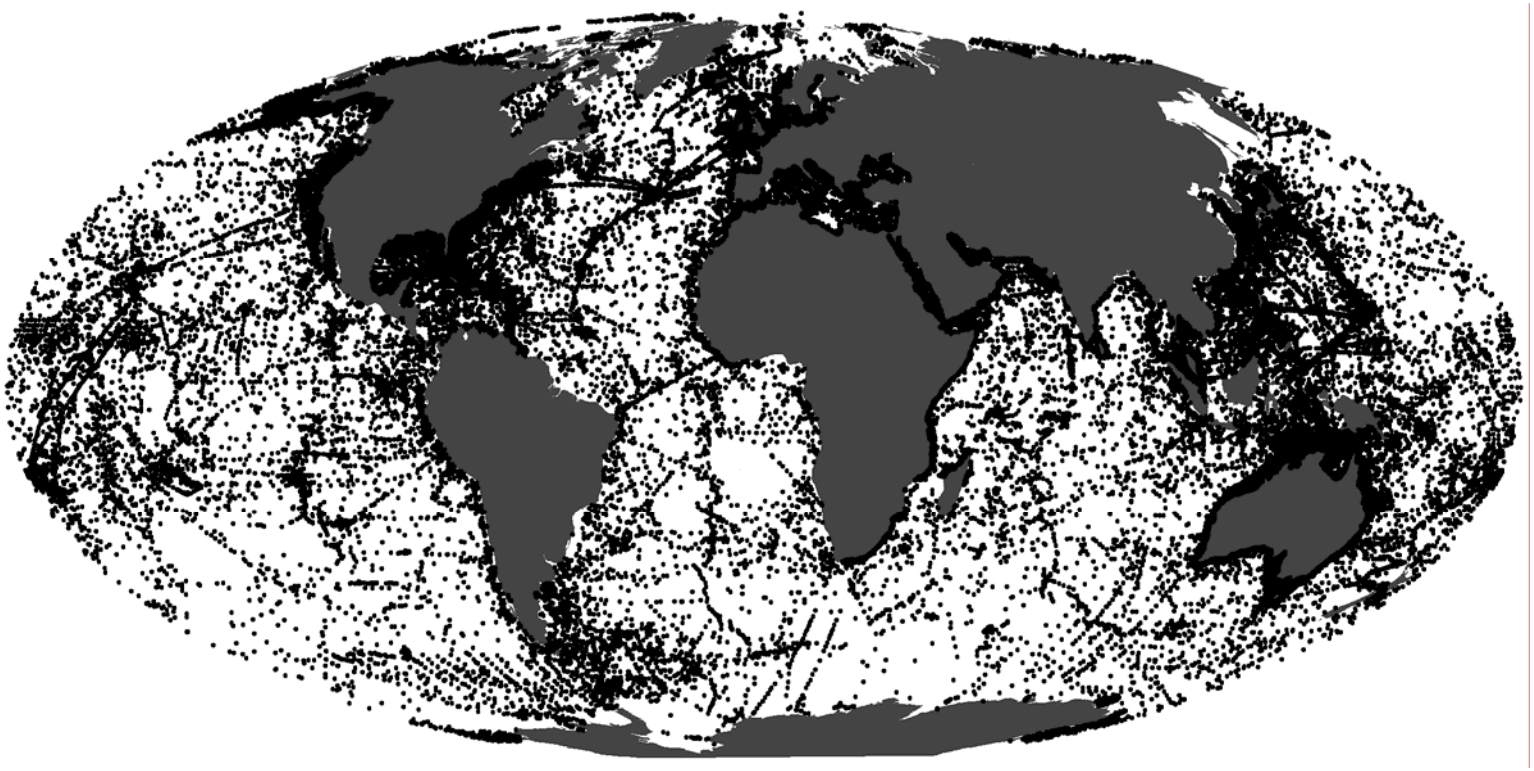

Supplementary Figure 5. Regression fits for average cumulative impact scores for 16 locations around the world in which overall current condition of coral reef-associated ecosystems were assessed (S*32*). Analyses were done A) across all ecosystems within cells that contained coral reefs, and B) coral reefs alone.

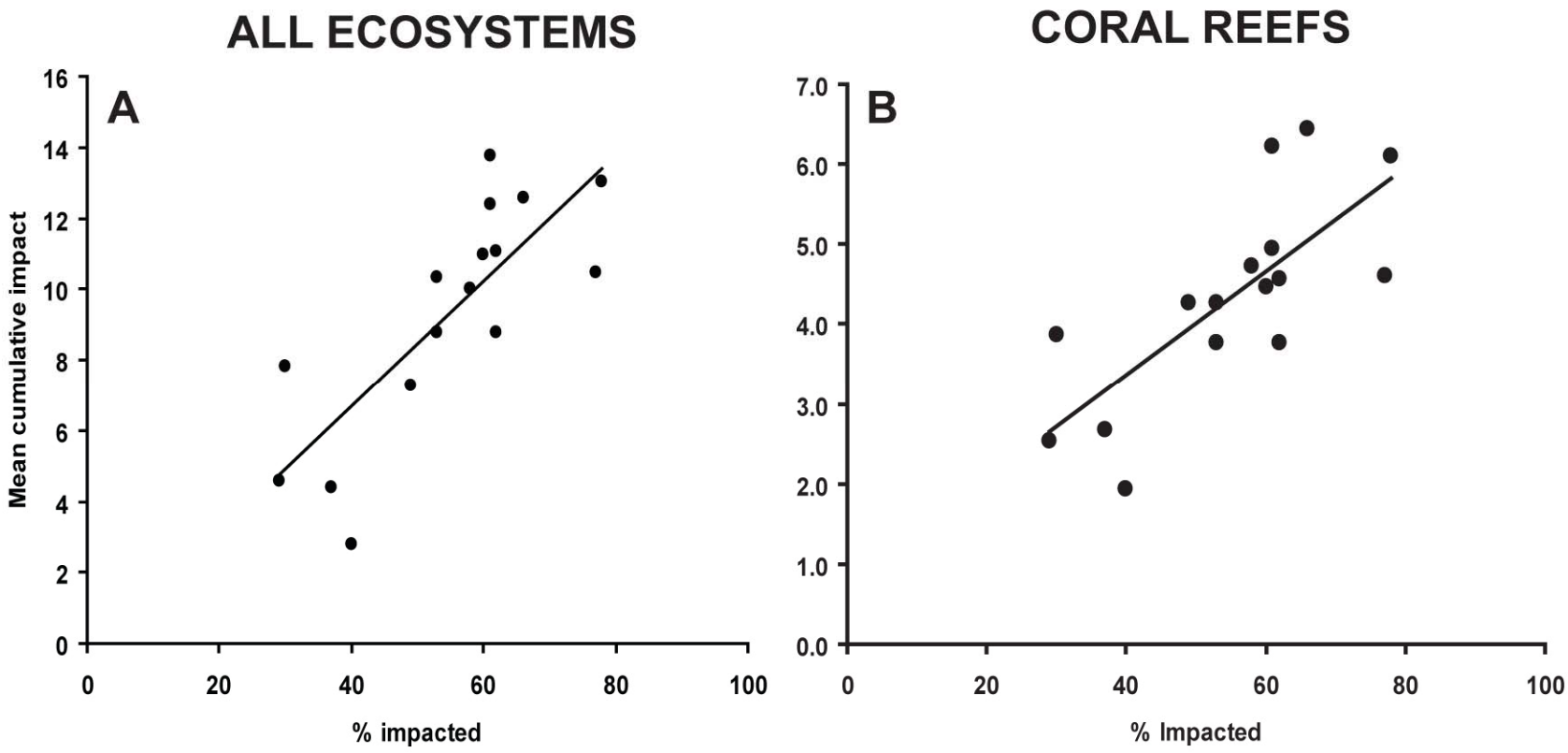

Supplementary Figure 6. Regional comparisons of cumulative impact scores for Southern California (A, B) and the coast of Portugal (C, D) for the full analyses presented in the manuscript (A, C) and with the 6 intertidal and shallow ecosystems removed with assumed distributions (B, D).

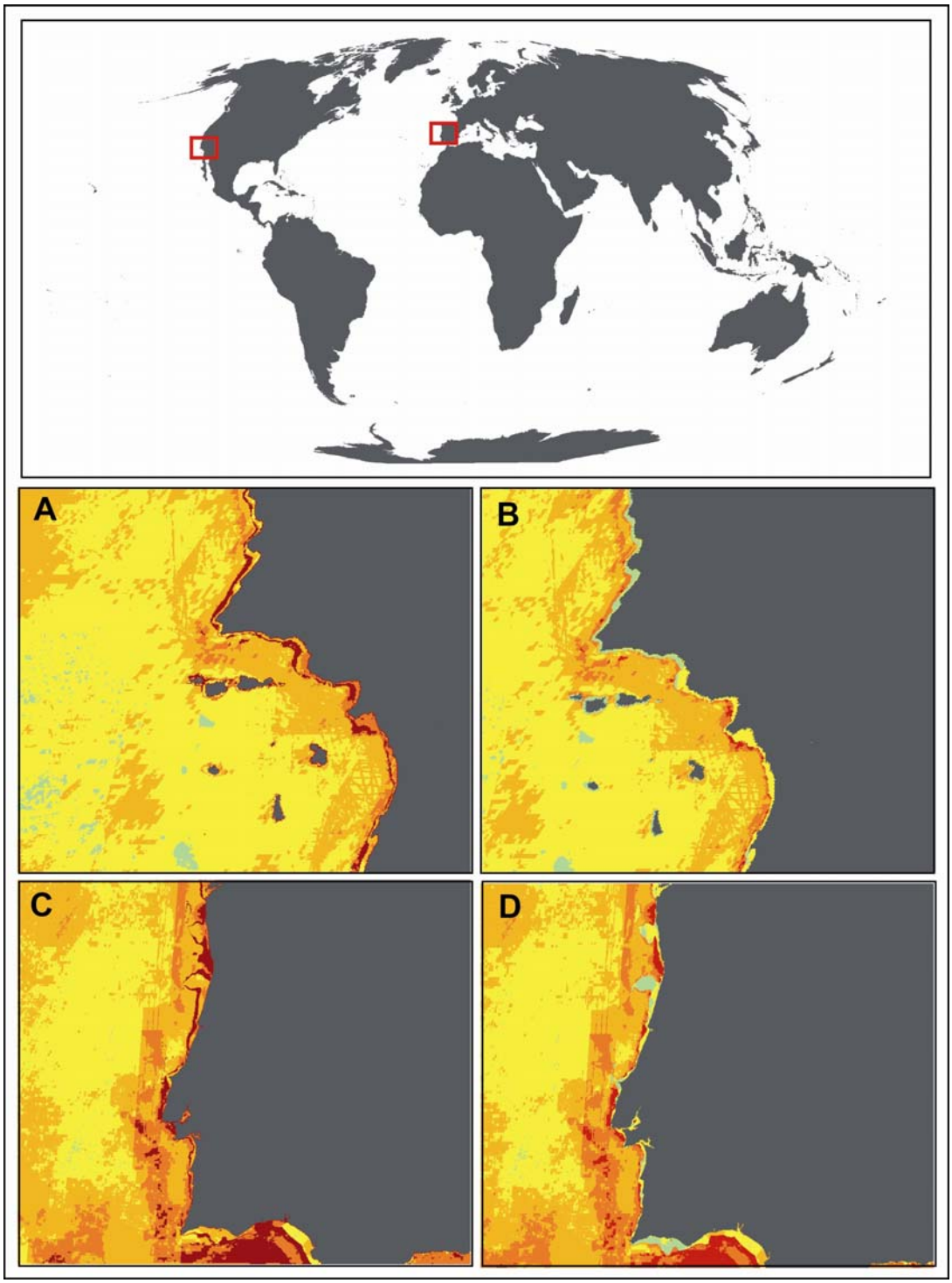

Supplementary Table 1. List of all driver data used in analyses with associated native resolution.

Data Layer	Native Resolution	Years Used
Drivers		
Nutrients (fertilizer)	1km^2	1993-2002
Organic pollutants (pesticides)	1km^2	1992-2001
Inorganic pollutants (impervious surfaces)	1km^2	2000-2001
Direct human (population density)	1km^2	2005
Pelagic, low-bycatch fishing	half-degree	1999-2003
Pelagic, high-bycatch fishing	half-degree	1999-2003
Demersal, destructive fishing	half-degree	1999-2003
Demersal, non-destructive, low-bycatch fishing	half-degree	1999-2003
Demersal, non-destructive, high-bycatch fishing	half-degree	1999-2003
Artisanal fishing	1km^2	1999-2003
Oil rigs	30 arc-second (~1km^2)	2003
Invasive species	1km^2	1999-2003
Ocean pollution	1km^2	1999-2003, 2004-2005
Shipping	lat/long data	2004-2005
SST	21km^2	1985-2005
UV	1 degree	1996-2004
Ocean acidification	1 degree	1870 vs. 2000-2009
Ecosystems		**Year Accessed**
Coral	1:250000	2006
Seagrass	1:250000	2006
Mangrove	1:250000	2006
Rocky reef	lat/long data combined with 2 minute bathymetry	2005
Shallow soft	lat/long data combined with 2 minute bathymetry	2005
Hard shelf	lat/long data combined with 2 minute bathymetry	2005
Soft shelf	lat/long data combined with 2 minute bathymetry	2005
Hard slope	lat/long data combined with 2 minute bathymetry	2005
Soft slope	lat/long data combined with 2 minute bathymetry	2005
Hard deep	lat/long data combined with 2 minute bathymetry	2005
Soft deep	lat/long data combined with 2 minute bathymetry	2005
Seamounts	14,287 point data with lat/long	2004
Pelagic waters	derived from 2 minute bathymetry	2006
Deep waters	derived from 2 minute bathymetry	2006

Supplementary Table 2. Matrix of driver-by-ecosystem impact weighting values from (S*1*).

Driver	Mangrove	Coral Reef	Seagrass	Rocky Reef	Sub-tidal Soft Bottom	Soft Shelf (30-200m)	Hard Shelf (30-200m)	Soft Slope (200-2000m)	Hard Slope (200-2000m)	Deep Soft Benthic	Deep Hard Bottom	Deep Seamount	Surface Water	Deep Water	Rocky Intertidal	Intertidal Mud	Beach	Salt Marsh	Kelp Forest	Susp.-Feeder Reef
Nutrient Input	1.8	1.8	2.1	1.6	2.0	1.4	1.7	2.0	0.6	1.3	0.0	0.0	1.2	0.0	1.5	1.6	0.4	1.8	0.4	1.4
Nonpoint, organic pollution	1.4	1.2	1.0	2.2	1.2	1.4	0.0	2.0	0.2	1.7	0.0	0.0	1.9	1.6	2.1	2.8	0.1	1.7	1.0	2.8
Nonpoint, non-organic pollution	0.5	0.7	0.8	2.2	1.5	2.1	0.2	2.1	0.2	1.8	0.0	0.0	2.3	1.6	2.1	1.6	0.6	2.0	0.0	2.7
Direct Human	3.3	2.3	2.5	2.5	2.0	1.1	2.9	0.0	0.0	1.6	0.0	0.0	0.9	0.0	2.8	2.2	2.7	1.6	1.6	3.0
Demersal, destructive fishing	0.0	1.2	0.2	2.7	2.1	3.0	3.1	3.2	2.8	2.3	3.0	3.5	2.1	0.8	1.2	1.4	0.2	1.0	1.5	3.1
Demersal, non-destructive, high bycatch fishing	0.9	1.6	1.1	2.9	2.1	2.0	3.2	2.3	2.4	2.0	0.0	0.0	1.6	0.0	0.8	1.9	0.9	1.0	2.1	0.7
Demersal, non-destructive, low bycatch fishing	0.8	1.3	0.6	2.7	1.7	1.6	2.6	0.0	2.2	0.0	0.0	0.0	0.0	0.0	1.5	1.5	0.2	0.5	2.1	1.4
Pelagic, high by-catch fishing	0.0	0.5	0.0	2.6	0.0	1.1	2.8	0.2	0.0	1.6	0.0	0.0	3.0	2.2	0.9	0.0	0.1	0.5	0.0	0.0
Pelagic, low by-catch fishing	0.0	0.7	0.0	2.6	0.6	0.8	2.8	0.2	0.0	0.5	0.0	0.0	2.2	0.6	0.0	0.0	0.0	0.4	0.0	0.0
Artisanal fishing	1.7	2.3	0.3	2.2	0.0	0.9	1.9	0.0	0.4	0.3	0.0	0.9	1.0	0.0	1.3	0.4	0.7	0.6	0.8	1.0
Sea temperature	2.4	2.8	2.1	1.9	0.5	2.5	2.9	2.3	0.9	2.5	1.5	1.8	3.3	2.3	2.8	1.4	0.6	1.4	2.0	0.8
UV	0.2	0.8	0.5	0.7	0.3	1.9	1.8	0.0	0.0	1.3	0.0	0.0	1.5	0.0	0.9	1.3	0.0	1.1	0.1	0.0
Ocean acidification	1.2	1.1	1.4	1.1	0.1	1.7	2.5	2.1	1.6	2.2	2.7	2.7	1.8	0.0	0.9	1.0	0.0	1.3	0.0	0.7
Species Invasion	1.0	1.5	1.2	2.5	2.7	1.6	1.5	0.2	0.5	1.5	0.0	0.0	2.3	0.0	2.8	2.9	0.9	2.8	1.3	2.6
Ocean-based pollution	1.2	1.2	0.5	1.7	1.1	1.2	0.3	1.4	1.7	2.3	1.2	1.2	1.7	0.4	1.3	0.8	0.5	1.2	0.1	0.0
Commercial Activity	2.0	1.5	1.9	1.4	0.3	1.7	0.9	0.1	1.0	0.9	0.0	0.0	1.9	0.0	0.3	1.9	1.9	1.4	0.0	0.0
Benthic Structures	1.3	0.5	1.6	1.7	0.1	0.5	2.1	1.6	2.2	1.9	1.6	1.4	1.5	0.0	1.0	0.9	0.8	0.9	0.0	0.4

Supplementary Table 3. The overall size (km^2) and minimum (Min), maximum (Max), mean (Mean), and sum total (Sum) cumulative impact score across all cells within each marine ecoregion (S*36*). Ecoregions are listed by realms.

Realm	Code	Ecoregion	Km2	Min	Max	Mean	Sum
ARCTIC							
	1	North Greenland	159,781	0.0	20.1	3.2	512,880
	2	North and East Iceland	33,370	0.5	46.5	14.3	478,339
	3	East Greenland Shelf	136,231	0.1	26.1	5.0	683,930
	4	West Greenland Shelf	186,225	0.0	37.5	8.6	1,602,940
	5	Northern Grand Banks, Southern Labrador	150,479	0.7	54.7	12.1	1,824,770
	6	Northern Labrador	130,230	0.1	29.1	6.9	894,741
	7	Baffin Bay - Davis Strait	58,795	0.0	19.0	3.4	197,892
	8	Hudson Complex	1,282,996	0.0	39.3	4.2	5,359,070
	9	Lancaster Sound	195,622	0.0	15.7	1.9	377,207
	10	High Arctic Archipelago	166,522	0.0	18.5	2.6	435,680
	11	Beaufort-Amundsen-Viscount Melville-	332,032	0.0	21.7	2.6	851,292
	12	Beaufort Sea - continental coast and shelf	119,134	0.1	20.9	2.2	256,827
	13	Chukchi Sea	627,245	0.0	23.3	3.6	2,233,820
	14	Eastern Bering Sea	1,026,502	0.1	40.1	8.8	9,073,790
	15	East Siberian Sea	1,026,378	0.0	21.0	1.9	1,920,860
	16	Laptev Sea	566,653	0.0	27.3	1.6	894,508
	17	Kara Sea	838,528	0.0	35.4	3.0	2,544,360
	18	North and East Barents Sea	863,044	0.1	24.1	6.2	5,311,840
	19	White Sea	97,672	0.3	42.4	6.9	673,061
TEMPERATE NORTHERN ATLANTIC							
	20	South and West Iceland	96,771	2.3	55.2	14.8	1,430,150
	21	Faroe Plateau	28,343	2.7	45.9	15.1	428,034
	22	Southern Norway	66,730	2.5	61.4	17.5	1,167,530
	23	Northern Norway and Finnmark	99,093	0.4	51.5	14.9	1,473,680
	24	Baltic Sea	413,619	0.4	68.2	9.1	3,774,150
	25	North Sea	701,559	0.8	81.2	12.4	8,695,670
	26	Celtic Seas	489,485	1.9	61.5	14.0	6,842,880
	27	South European Atlantic Shelf	151,870	1.3	72.3	11.8	1,797,340
	28	Saharan Upwelling	128,407	0.3	63.9	9.3	1,197,950
	29	Azores Canaries Madeira	8,934	0.6	67.5	15.5	138,080
	30	Adriatic Sea	117,672	0.9	59.4	12.1	1,420,020
	31	Aegean Sea	85,713	1.0	57.7	13.7	1,178,550
	32	Levantine Sea	63,563	0.5	57.0	11.4	724,402
	33	Tunisian Plateau/Gulf of Sidra	129,305	0.7	48.6	11.0	1,416,220
	34	Ionian Sea	45,973	1.1	73.0	14.3	659,668
	35	Western Mediterranean	122,459	1.4	70.8	13.5	1,649,190
	36	Alboran Sea	12,686	2.3	56.7	13.9	176,692
	37	Gulf of St. Lawrence, Eastern Scotian Shelf	244,322	0.9	54.0	11.3	2,760,440
	38	Southern Grand Banks - South	267,422	1.0	43.9	11.4	3,055,600
	39	Scotian Shelf	116,817	2.3	47.5	13.1	1,531,530
	40	Gulf of Maine/Bay of Fundy	133,702	2.8	62.5	13.2	1,764,760
	41	Virginian	171,626	0.9	64.4	11.1	1,900,710
	42	Carolinian	115,186	0.7	45.1	6.2	711,282
	43	Northern Gulf of Mexico	288,688	0.7	57.0	6.5	1,889,980
	44	Black Sea	161,176	0.7	59.7	9.6	1,550,430
TEMPERATE NORTHERN PACIFIC							
	45	Sea of Okhotsk	541,588	0.6	42.7	7.0	3,811,460
	46	Kamchatka Shelf and Coast	87,954	0.1	35.8	6.7	590,041
	47	Oyashio Current	56,177	0.5	53.1	9.6	537,950
	48	Northeastern Honshu	30,572	2.3	70.3	13.8	422,224
	49	Sea of Japan	182,664	0.9	71.3	12.6	2,303,360
	50	Yellow Sea	496,651	0.6	61.2	9.3	4,624,850
	51	Central Kuroshio Current	78,821	2.1	69.0	15.1	1,188,660
	52	East China Sea	637,621	1.3	72.2	13.7	8,718,290
	53	Aleutian Islands	56,547	0.2	42.9	10.0	563,070
	54	Gulf of Alaska	266,148	0.6	48.2	12.3	3,273,330
	55	North American Pacific Fijordland	108,818	0.6	45.7	12.1	1,312,610
	56	Puget Trough/Georgia Basin	13,694	2.7	66.1	19.3	264,029
	57	Oregon, Washington, Vancouver Coast	55,645	1.6	53.0	12.5	696,947
	58	Northern California	22,298	2.2	61.1	11.7	260,997
	59	Southern California Bight	41,843	0.9	49.2	7.3	307,048
	60	Cortezian	100,026	0.3	48.6	8.3	834,683
	61	Magdalena Transition	28,417	1.0	40.6	5.6	159,730

TROPICAL ATLANTIC						
62	Bermuda	1,079	2.2	50.3	10.3	11,153
63	Bahamian	130,055	0.4	52.4	5.6	729,903
64	Eastern Caribbean	25,050	1.1	89.6	13.9	349,068
65	Greater Antilles	94,671	0.5	72.3	10.4	988,269
66	Southern Caribbean	116,527	0.6	62.1	10.7	1,248,240
67	Southwestern Caribbean	162,099	0.5	75.9	7.4	1,206,590
68	Western Caribbean	32,499	0.5	65.1	11.0	357,435
69	Southern Gulf of Mexico	226,576	0.7	52.8	6.8	1,534,720
70	Floridian	138,094	0.7	64.8	7.9	1,085,980
71	Guianan	214,527	0.4	52.3	7.8	1,679,760
72	Amazonia	328,811	0.5	52.9	5.5	1,805,590
73	Sao Pedro and Sao Paulo Islands	[no area <200m in our bathymetry data for this ecoregion]				
74	Fernando de Naronha & Atoll das Rocas	379	1.1	35.0	7.7	2,903
75	Northeastern Brazil	85,887	0.8	49.2	5.5	473,161
76	Eastern Brazil	119,978	0.4	55.0	7.2	865,500
77	Trindade and Martin Vaz Islands	53	0.5	13.2	4.1	218
78	St. Helena and Ascension Islands	741	0.3	31.5	5.2	3,855
79	Cape Verde	5,470	0.3	46.3	10.1	55,246
80	Sahelian Upwelling	61,392	0.8	61.1	10.2	626,943
81	Gulf of Guinea West	147,819	0.6	61.7	8.4	1,235,250
82	Gulf of Guinea Upwelling	33,156	1.2	65.0	10.2	337,059
83	Gulf of Guinea Central	87,557	0.3	78.8	10.9	958,521
84	Gulf of Guinea Islands	2,049	0.3	39.0	7.0	14,438
85	Gulf of Guinea South	46,381	1.9	49.5	8.4	389,496
86	Angolan	39,996	1.3	62.1	10.6	422,312
WESTERN INDO-PACIFIC						
87	Northern and Central Red Sea	62,895	0.4	65.8	10.3	649,089
88	Southern Red Sea	164,592	0.3	69.2	7.1	1,160,630
89	Gulf of Aden	44,706	0.4	59.4	9.3	417,801
90	Arabian (Persian) Gulf	274,438	0.3	64.2	8.8	2,419,080
91	Gulf of Oman	50,117	0.6	52.9	9.4	473,233
92	Western Arabian Sea	55,244	0.5	38.6	6.7	368,475
93	Central Somali Coast	29,634	0.3	23.6	5.0	147,543
94	Northern Monsoon Current Coast	13,220	0.5	40.9	6.5	86,393
95	East African Coral Coast	41,080	0.8	54.7	8.1	333,032
96	Seychelles	45,354	0.3	38.5	5.1	229,741
97	Cargados Carajos/Tromelin Island	68,194	0.4	33.6	8.1	554,448
98	Mascarene Islands	4,058	0.5	61.6	10.9	44,330
99	Southeast Madagascar	25,122	0.6	42.6	7.5	187,684
100	Western & Northern Madagascar	82,356	0.3	62.4	6.6	546,478
101	Bight of Sofala/Swamp Coast	59,029	0.5	44.4	4.8	283,987
102	Delagoa	27,788	0.4	44.6	7.5	209,198
103	Western India	324,590	0.5	62.8	9.6	3,106,840
104	South India and Sri Lanka	73,843	1.4	73.7	10.6	780,347
105	Maldives	42,993	0.6	56.0	7.5	323,881
106	Chagos	23,799	0.3	31.9	3.5	84,074
107	Eastern India	44,442	1.7	66.1	11.0	487,431
108	Northern Bay of Bengal	236,470	0.8	60.9	7.6	1,807,480
109	Andaman and Nicobar Islands	43,376	1.4	61.4	10.6	461,808
110	Andaman Sea Coral Coast	176,070	1.3	61.4	8.6	1,513,680
111	Western Sumatra	78,046	0.6	54.3	8.5	664,370
CENTRAL INDO-PACIFIC						
112	Gulf of Tonkin	237,412	0.3	65.5	9.4	2,232,290
113	Southern China	250,718	1.6	82.8	12.6	3,159,500
114	South China Sea Oceanic Islands	31,514	1.1	40.1	11.9	373,511
115	Gulf of Thailand	309,917	1.0	54.9	8.1	2,495,570
116	Southern Vietnam	126,279	1.4	62.9	6.1	769,969
117	Sunda Shelf	1,498,388	0.5	70.1	8.3	12,401,600
118	Malacca Strait	153,794	0.8	90.1	10.5	1,608,470
119	Southern Java	59,663	0.7	55.7	8.2	488,623
120	Cocos-Keeling/Christmas Island	849	0.4	44.1	10.8	9,205
121	South Kuroshio Current	29,404	0.7	80.8	14.8	435,888
122	Ogasawara Islands	2,751	1.0	37.7	12.3	33,939
123	Mariana Islands	1,598	0.6	70.3	15.8	25,219
124	East Caroline Islands	20,344	0.3	52.0	6.1	123,333
125	West Caroline Islands	5,912	0.3	42.9	7.5	44,368
126	Palawan/North Borneo	234,118	0.7	68.6	10.2	2,387,730
127	Eastern Philippines	145,657	1.1	83.3	14.5	2,108,290
128	Sulawesi Sea/Makassar Strait	190,983	0.8	64.2	6.6	1,260,800
129	Halmahera	36,534	1.2	58.2	7.8	285,806
130	Papua	116,385	0.5	55.9	6.6	765,091
131	Banda Sea	105,507	0.7	62.4	7.6	797,988
132	Lesser Sunda	44,694	0.4	67.4	11.2	501,357
133	Northeast Sulawesi	30,354	0.5	41.6	6.0	183,267

	134 Bismarck Sea	30,890	0.4	49.7	9.8	303,154
	135 Solomon Archipelago	45,421	0.5	52.3	10.0	454,299
	136 Solomon Sea	70,248	0.4	47.3	5.1	356,485
	137 Southeast Papua New Guinea	8,644	0.3	49.4	4.7	40,898
	138 Gulf of Papua	55,067	0.3	27.8	3.3	180,940
	139 Arafura Sea	405,761	0.4	37.4	4.6	1,875,440
	140 Arnhem Coast to Gulf of Carpenteria	664,520	0.3	37.1	3.4	2,247,190
	141 Bonaparte Coast	374,406	0.3	36.1	4.2	1,579,840
	142 Torres Strait Northern Great Barrier Reef	112,705	0.4	32.3	1.8	199,838
	143 Central and Southern Great Barrier Reef	220,909	0.4	55.3	4.5	992,977
	144 Exmouth to Broome	331,774	0.4	47.3	6.6	2,178,090
	145 Ningaloo	9,248	0.5	27.0	3.9	36,141
	146 Tonga Islands	8,561	0.6	53.7	13.0	111,182
	147 Fiji Islands	47,278	0.3	63.0	8.4	398,900
	148 Vanuatu	12,457	0.4	59.9	13.8	172,016
	149 New Caledonia	65,987	0.3	43.5	4.4	288,666
	150 Coral Sea	15,067	0.4	23.2	3.6	54,247
	151 Lord Howe and Norfolk Islands	5,313	0.4	24.7	5.3	28,218
EASTERN INDO-PACIFIC						
	152 Hawaiian Islands	19,314	0.6	68.5	11.4	220,271
	153 Marshall Islands	22,067	0.4	58.8	7.7	168,913
	154 Gilbert/Ellis Islands	12,097	0.4	47.5	9.0	109,059
	155 Line Islands	2,117	0.3	35.7	7.1	15,027
	156 Phoenix/Tokelau/Northern Cook Islands	1,456	0.3	34.8	11.3	16,396
	157 Samoa Islands	3,787	0.7	62.0	15.7	59,451
	158 Tuamotus	27,811	0.4	38.9	7.0	195,621
	159 Rapa-Pitcairn	388	0.3	24.6	6.8	2,637
	160 Southern Cook/Austral Islands	1,311	0.3	40.7	9.6	12,524
	161 Society Islands	1,904	0.6	62.2	19.5	37,074
	162 Marquesas	1,687	0.3	25.9	7.0	11,850
	163 Easter Island	312	0.6	29.1	10.3	3,207
TROPICAL EASTERN PACIFIC						
	164 Revillagigedos	280	1.1	22.5	8.8	2,476
	165 Clipperton	26	0.5	19.4	8.4	217
	166 Mexican Tropical Pacific	12,324	1.0	40.8	9.7	119,787
	167 Chiapas-Nicaragua	93,545	0.5	50.6	8.0	752,905
	168 Nicoya	25,636	0.8	52.8	10.8	276,997
	169 Cocos Islands	355	1.8	8.4	4.3	1,531
	170 Panama Bight	57,601	0.3	51.3	8.2	471,271
	171 Guayaquil	28,175	1.9	53.6	8.6	242,709
	172 Northern Galapagos Islands	59	0.3	10.0	4.0	236
	173 Eastern Galapagos Islands	8,734	0.3	30.7	6.8	59,053
	174 Western Galapagos Islands	1,448	0.6	26.0	6.4	9,311
TEMPERATE SOUTH AMERICA						
	175 Central Peru	62,881	1.3	63.9	8.8	555,180
	176 Humboldtian	24,252	1.7	58.2	11.6	281,685
	177 Central Chile	7,392	3.2	60.6	15.3	113,408
	178 Araucanian	29,755	2.1	65.3	9.9	295,681
	179 Juan Fernández and Desventuradas	839	1.3	27.5	7.5	6,317
	180 Southeastern Brazil	171,877	0.7	60.4	10.8	1,859,740
	181 Rio Grande	111,577	0.6	34.6	8.4	937,479
	182 Rio de la Plata	35,908	0.7	55.4	5.5	196,355
	183 Uruguay-Buenos Aires Shelf	287,165	0.6	47.3	7.4	2,137,920
	184 North Patagonian Gulfs	238,505	0.5	32.8	7.9	1,887,870
	185 Patagonian Shelf	450,549	0.3	29.0	9.0	4,071,890
	186 Malvinas/Falklands	174,680	0.2	29.8	7.6	1,324,870
	187 Channels and Fjords of Southern Chile	130,971	0.3	41.7	6.5	852,807
	188 Chiloense	53,113	0.8	41.6	7.8	414,000
	189 Tristan Gough	3,884	0.3	23.7	2.5	9,544
TEMPERATE SOUTHERN AFRICA						
	190 Namib	66,223	0.6	37.3	9.7	643,684
	191 Namaqua	92,157	0.5	59.7	8.8	814,549
	192 Agulhas	102,706	1.5	47.0	9.7	999,498
	193 Natal	17,841	1.1	59.0	12.2	217,407
	194 Amsterdam-St Paul	153	0.5	22.0	7.9	1,213

TEMPERATE AUSTRALASIA						
195	Kermadec Island	442	0.7	22.3	7.6	3,355
196	Northeastern New Zealand	38,384	0.6	48.6	7.8	300,180
197	Three Kings-North Cape	5,847	1.1	28.8	6.2	36,513
198	Chatham Island	13,456	0.4	20.4	3.7	50,393
199	Central New Zealand	156,804	0.7	53.2	8.3	1,295,080
200	Southern New Zealand	36,768	0.6	44.5	7.5	275,369
201	Snares Island	17,068	0.7	10.7	4.1	69,548
202	Tweed-Moreton	46,833	0.4	68.4	9.1	427,644
203	Manning-Hawkesbury	21,322	0.8	67.3	13.7	291,050
204	Cape Howe	67,531	0.4	54.2	9.6	647,988
205	Bassian	108,318	0.4	55.9	10.4	1,122,520
206	Western Bassian	78,842	0.6	60.5	9.1	718,220
207	South Australian Gulfs	111,434	0.6	63.5	8.7	973,032
208	Great Australian Bight	162,322	0.5	31.7	7.0	1,131,740
209	Leeuwin	80,382	0.6	58.2	7.7	617,591
210	Shark Bay	59,401	0.5	35.3	4.6	275,882
211	Houtman	36,512	0.7	54.7	5.8	212,049
SOUTHERN OCEAN						
212	Macquarie Island	538	0.2	18.1	4.2	2,275
213	Heard and Macdonald Islands	7,375	0.2	16.3	6.0	43,947
214	Kerguelen Islands	71,148	0.2	16.2	6.4	454,815
215	Crozet Islands	7,898	2.0	19.3	7.4	58,377
216	Prince Edward Islands	792	1.3	19.4	6.7	5,280
217	Bouvet Island	187	1.0	15.8	4.5	850
218	Peter the First Island	476	0.1	6.0	1.0	452
219	South Sandwich Islands	1,120	0.2	15.8	3.1	3,436
220	South Georgia	25,644	0.2	19.2	3.6	92,534
221	South Orkney Islands	8,954	0.2	8.6	2.9	26,331
222	South Shetland Islands	20,922	0.2	9.7	3.3	69,729
223	Antarctic Peninsula	173,262	0.0	11.0	1.2	208,317
224	East Antarctic Wilkes Land	342,217	0.0	10.1	1.3	451,073
225	East Antarctic Enderby Land	15,859	0.0	7.7	1.9	30,916
226	East Antarctica Dronning Maud Land	169,058	0.0	8.4	0.6	104,514
227	Weddell Sea	839,466	0.0	8.3	0.2	171,039
228	Amundsen/Bellingshausen Sea	375,442	0.0	8.1	0.8	297,402
229	Ross Sea	704,730	0.0	8.2	0.1	79,758
230	Bounty and Antipodes Islands	5,793	0.3	17.9	2.1	12,295
231	Campbell Island	10,384	0.6	21.6	6.7	69,094
232	Auckland Island	14,611	0.8	23.0	5.1	75,017

Supplementary Table 4. List of gear types classified into each of the 5 types of commercial fishing mapped in this project.

Pelagic, low-bycatch	Pelagic, high-bycatch	Demersal, destructive	Demersal, non-destructive, low-bycatch	Demersal, non-destructive, high-bycatch
*troll lines (hook and line	*driftnets (gillnet)	*bomb/chemical (all types)	*castnets (all types)	*gillnet fixed (gillnet)
*squid hooks (hook and line)	*set lines (hook and line)	*bottom trawl (all types)	*hand (all types)	*gillnet encircling (gillnet)
*liftnet (all types)	*drift lines (hook and line)	*dredge (all types)	*spear (all types)	*seine (seine)
*net (all types)	*midwater trawl (all types)		*gorges and hooks (hook and line; for demersal species)	*beach seine (seine)
*lampara-like (seine)			*handlines (hook and line; for demersal species)	*boat seine (seine)
*purse seine (seine)			*lines (hook and line; for demersal species)	*trammel (all types)
*ring seine (seine)			*pilks or jigs (hook and line; for pelagic species)	*trap (all types)
*gorges and hooks (hook and line; for pelagic species)				
*handlines (hook and line; for pelagic species)				
*lines (hook and line; for pelagic species)				
*pilks or jigs (hook and line; for pelagic species)				

Supplementary Table 5. Percent of each marine ecosystem lost when clipped to land-sea mask.

Ecosystem	% change in area
coral reef	-12.3
mangrove	-91.7
seagrass	-8.4
rocky reef	-0.007
shallow soft bottom	-0.003
hard shelf	0.0
soft shelf	0.0
hard slope	0.0
soft slope	0.0
hard deep	0.0
soft deep	0.0
seamounts	0.0
pelagic waters	0.0
deep waters	0.0

Supplementary Table 6. Classification scheme for ocean condition categories (including % degradation ranges from (*S10, 34*)), range of cumulative impact scores and amount of ocean (km^2 and %) associated with each category, and mean percent of ocean +/- 95% CI for each anthropogenic driver category derived from Monte-Carlo simulations (see SOM).

					Monte-Carlo Simulations	
Ocean Condition	**% degraded**	**Cumulative impact scores**	**# cells (~km2)**	**% of oceans**	**Mean**	**95%CI**
no impact		0	0	0	0	
very low impact	<10	0.0 - 1.42	15,300,901	3.7	4.4	+/- 0.4
low impact	10-30	1.42 - 4.95	101,942,172	24.5	25.3	+/- 1.7
medium impact	30-50	4.95 - 8.47	130,429,789	31.3	42.3	+/- 1.3
medium high impact	50-70	8.47 - 12.00	159,117,800	38.2	22.8	+/- 1.4
high impact	70-90	12.00 - 15.52	7,514,421	1.8	4.4	+/- 0.6
very high impact	>90	15.53 - 90.07	2,240,935	0.5	0.7	+/- 0.1

References

S1. B. S. Halpern, K. A. Selkoe, F. Micheli, C. V. Kappel, *Conservation Biology* 21, 1301 (2007).

S2. S. K. Jenson, J. O. Domingue, *Photogrammetric Engineering and Remote Sensing* 54, 1593 (1988).

S3. NIMA, "Vector Map Level 0 (VMAP0)" (National Imagery and Mapping Agency, 1997).

S4. P. Wessel, W. H. F. Smith, *Journal of Geophysical Research* 101, 8741 (1996).

S5. J. Mennis, T. Hultgren, *Cartography and Geographic Information Science* 13, 179 (2006).

S6. J. Xu, R. Lathrop, *International Journal of Geographic Information Science* 9, 153 (1995).

S7. R. Watson, C. Revenga, Y. Kura, *Fisheries Research* 79, 97 (2006).

S8. R. Watson, A. Kitchingman, A. Gelchu, D. Pauly, *Fish and Fisheries* 5, 168 (2004).

S9. M. J. Behrenfeld, P. G. Falkowski, *Limnology And Oceanography* 42, 1 (Jan, 1997).

S10. J. B. C. Jackson *et al.*, *Science* 293, 629 (Jul 27, 2001).

S11. K. T. Frank, B. Petrie, J. S. Choi, W. C. Leggett, *Science* 308, 1621 (Jun 10, 2005).

S12. M. H. Graham, *Ecology* 84, 2809 (Nov, 2003).

S13. D. Zeller, S. Booth, P. Craig, D. Pauly, *Coral Reefs* 25, 144 (Mar, 2006).

S14. ISL, "Ownership patterns of the world merchant fleet" (Institute of Shipping Economics and Logistics, 2005).

S15. J. M. Drake, D. M. Lodge, *Proceedings Of The Royal Society Of London Series B-Biological Sciences* 271, 575 (Mar 22, 2004).

S16. J. T. Carlton, J. B. Geller, *Science* 261, 78 (Jul 2, 1993).

S17. LLPOTW, "Lloyds List ports of the world" (Informa UK Ltd, 2003).

S18. L. M. Herborg, C. L. Jerde, D. M. Lodge, G. M. Ruiz, H. J. MacIsaac, *Ecological Applications* 17, 663 (Apr, 2007).

S19. G. Liu, W. J. Skirving, A. E. Strong, *EOS* 84, 137 (2003).

S20. R. Berkelmans, G. De'ath, S. Kininmonth, W. J. Skirving, *Coral Reefs* 23, 74 (Apr, 2004).

S21. R. D. McPeters, P. K. Bhartia, A. J. Krueger, O. Torres, J. R. Herman, "Earth Probe Total Ozone Mapping Spectrometer (TOMS) Data Products User's Guide" *Tech. Report No. NASA Technical Publication 1998-206895* (NASA, 1998).

S22. J. A. Kleypas *et al.*, *Science* 284, 118 (1999).

S23. J. M. Guinotte, R. W. Buddemeier, J. A. Kleypas, *Coral Reefs* 22, 551 (2003).

S24. J. Malczewski, *Transactions in GIS* 4, 5 (2000).

S25. D. O'Sullivan, D. J. Unwin, *Geographic Information Analysis* (Wiley, Hoboken, NJ, 2003), pp.

S26. M. D. Spalding, C. Ravilious, E. P. Green, *World Atlas of Coral Reefs* (University of California Press, Berkeley, USA, 2001), pp.

S27. D. Bryant, L. Burke, J. McManus, M. Spalding, "Reefs at risk: a map-based indicator of threats to the world's coral reefs" (World Resources Institute, 1998).
S28. E. P. Green, F. T. Short, *World Atlas of Seagrasses* (University of California Press, Berkeley, USA, 2003), pp.
S29. M. D. Spalding, F. Blasco, C. D. Field, *World mangrove atlas* (International Society for Mangrove Ecosystems, Okinawa, Japan, 1997), pp.
S30. A. Kitchingman, S. Lai, in *Seamounts: biodiversity and fisheries* D. Pauly, T. Morato, Eds. (Fisheries Center Research Reports, Vancouver, B.C., 2004), vol. 12, pp. 7-12.
S31. R. S. Steneck *et al.*, *Environmental Conservation* 29, 436 (Dec, 2002).
S32. J. M. Pandolfi *et al.*, *Science* 307, 1725 (2005).
S33. J. M. Pandolfi *et al.*, *Science* 301, 955 (Aug 15, 2003).
S34. H. K. Lotze *et al.*, *Science* 312, 1806 (Jun 23, 2006).
S35. R. B. Aronson *et al.*, *Science* 302, 1502 (2003).
S36. M. D. Spalding *et al.*, *Bioscience* 57, 573 (2007).